Solutions to Various Problems in Reversible Cooling fMRI Studies

by

Mark Haig Khachaturian

B.S.E Nuclear Engineering
B.S.E. Engineering Physics
University of Michigan, Ann Arbor, 2001

SUBMITTED TO THE DEPARTMENT OF NUCLEAR ENGINEERING IN PARTIAL FULFILLMENT OF THE REQUIREMENTS FOR THE DEGREE OF

MASTER OF SCIENCE IN NUCLEAR ENGINEERING
AT THE
MASSACHUSETTS INSTITUTE OF TECHNOLOGY

JULY 28, 2003

Signature of Author: _____
Department of Nuclear Engineering
July 28, 2003

Certified by: _____
Wim Vanduffel
Instructor
Harvard University, Cambridge, MA
Thesis Supervisor

Certified by: _____
Jacquelyn Yanch
Professor of Nuclear Engineering
MIT, Cambridge, MA
Thesis Reader

Accepted by: _____
Jeffrey Coderre
Associate Professor of Nuclear Engineering
Chairmen of the Department of the Committee of Graduate Students

Solutions to Various Problems in Reversible Cooling fMRI Studies

by

Mark Haig Khachaturian

Submitted to the Department of Nuclear Engineering in partial fulfillment of the requirements for the degree of Master of Science in Nuclear engineering at the Massachusetts Institute of Technology

July 28, 2003

ABSTRACT

Functional magnetic resonance imaging (fMRI) has been very useful in helping neuroscientists map the brain. One tool to investigate the interactions between brain regions is to disable a small region in the brain, and look at the functional consequences of this (reversible) inactivation upon regions anatomically connected to the inactivated site. A number of issues need to be resolved before the reversible cooling technique can be used in fMRI studies. The solutions to a number of problems directly related to using reversible inactivation by cooling in conjunction with fMRI experiments on monkey brains are presented in this thesis. Specifically, these include (1) designing a cooling system and cooling probe capable of reversibly cooling the surface cortex of the monkey's brain, (2) develop or use an existing method to measure the temperature distribution with the MR-scanner, and (3) design and construct a coil (phase array) that will be used to obtain temperature and fMRI data at the highest resolution possible. A cooling system and coolant probe were designed capable of changing the temperature of the surface cortex from 37 ^{o}C to 20 ^{o}C. The Proton Resonance Frequency Shift method, which calculates the temperature based on the phase change between two images, was used to measure the temperature distribution inside an object using an fMRI sequence similar to the one that will be used in the actual experiment. The method was tested and showed an accuracy of ± 0.6 ^{o}C as compared with concurrent thermocouple measurements when adjusted for phase drift. A precision of ± 0.15 ^{o}C was found at a resolution of 2.1 x 2.1 x 1.0 mm^{3}. A phase array head coil was designed with superior imaging qualities to the current single coil. An increase of SNR from 40 to 52 was observed in the image (30% increase) as compared with the theoretical calculated increase of 70%.

Thesis Supervisor: Wim Vanduffel
Title: Instructor, Harvard University, Cambridge, MA

Thesis Reader: Jacquelyn Yanch
Title: Professor of Nuclear Engineering, MIT, Cambridge, MA

TABLE OF CONTENTS

LIST OF FIGURES

LIST OF TABLES

LIST OF ACYRONYMS AND DEFINITIONS

SNR – Signal To Noise Ratio
MRI – Magnetic Resonance Imaging
fMRI – Functional Magnetic Resonance Imaging
NMR – Nuclear Magnetic Resonance
NMRI – Nuclear Magnetic Resonance Imaging
PRF – Proton Resonance Frequency
ROI – Region of Interest
EPI – Echo Planar Imaging
FOV – Field of View
TE – Excitation Time
TR – Relaxation Time

Phase Array Coil – Term used to describe a coil for a MRI system that is made up of any number of individual coils that behaves like a single coil.
Echo Planar Imaging Sequence – Sequence that is used in fMRI studies. The sequence can take an image of an entire slice of an object in five seconds.

§1 INTRODUCTION

Since its development in the early nineties, functional magnetic resonance imaging (fMRI) has been very useful in helping neuroscientists map the brain (i.e. localizing brain regions involved in the processing of particular functions) [1,2]. For example, fMRI studies have shown which parts of the visual cortex are activated by various visual stimuli. These stimuli can test various aspects of vision (focusing, peripheral, etc.) and cognitive skills. Experiments on motor skills, in which the subject is asked to perform certain tasks based on the stimuli, have also been conducted using fMRI. The major advantage of fMRI is that it is a completely non-invasive technique that can be used to study functional properties of healthy and diseased human subjects. This greatly simplifies the experimental procedure and allows multiple experiments to be performed on single subjects. So far, neuroscientists have focused mainly on 'mapping' questions (revealing valuable modern phrenological information). However, besides knowing which brain areas are involved in the processing of a particular stimulus, or task, it is of great importance to know how brain regions interact with each other. In other words: what kind of calculations are performed in one area and what kind of information is transmitted to the other areas. One tool to investigate the interactions between brain regions is to disable a small region in the brain and look at the functional consequences of this (reversible) inactivation upon regions anatomically connected to the inactivated site [1-4].

Data from reversible inactivation experiments provide information that fills an important gap to assess neural assemblies. When a region in the brain is cooled below 20 ^{o}C it looses functionality since the neurons cannot transmit information to other neurons at this temperature. Using this method one can investigate adult plasticity effects: i.e. other brain regions might take over (partially) the functions normally carried out by the deactivated region, as is seen in patients after strokes [1]. This can greatly help neuroscientists by investigating and devising recovery strategies after a stroke. Studies like these have been done with cats and monkeys but not with dynamic imaging techniques which yielding detailed functional information throughout the brain. In most other combined functional-imaging/reversible inactivation studies, the animal needed to be sacrificed [4]. The slices were then imaged based on radiation emitted by a radionuclide initially injected [1]. More recently, optical imaging studies have been done using electrophysiology while regions of the visual cortex have been deactivated [5]. It is more advantageous to perform reversible inactivation experiments in combination with fMRI since the monkey could be kept alive and the brain could be deactivated and then reactivated multiple times in addition to obtaining relatively detailed temporal information. Another advantage of using fMRI along with reversible inactivation compared with other methods discussed above is the ability of fMRI to obtain a temperature distribution in an object. In all previous studies, a model of the brain was used to calculate the region of inactivation or a few thermocouples were placed at critical points. Using MRI techniques, it might be possible to obtain very accurate temporal temperature distributions which will define the region of inactivation in a more quantitative fashion.

A number of problems need to be solved before reversible cooling can be used in fMRI studies. First of all, it is necessary to design a cooling system that is capable of reversible inactivation and to find a magnet-compatible and bio-compatible material that can be placed in the brain (coolant probe) through which the cooling fluid can flow without affecting the image quality.

A number of reversible inactivation methods have been explored. Malpeli (1999) describes the setup for reversible deactivation with a variety of pharmacological and chemical agents used in conjunction with electrophysiological assays of neural function [6]. Also, procedures have been described using pressure injection of the chemical GABA (gamma-amino butyric acid) to reversibly deactivate sites in the cerebral cortex [7]. In addition, a 'cryoloop', which consists of exceedingly thin (~ OD 0.6 mm) steel tubing, was implanted in cat brains. Super cooled ethanol (< -40 ^{o}C) flowed through the loop and cooled various regions in the cortex [1]. Of the reversible deactivation methods described above, the 'cryoloop' is the most compatible with fMRI. The difficulty of using chemical agents to inactivate the brain is the region of inactivation cannot be accurately measured during the experiment. Only models based on the diffusive properties of the chemicals can predict the region of inactivation. Temperature measurements are possible with fMRI and thus reversible inactivation by cooling provides experimentalists with the opportunity to obtain a thermal map while the experiment is being performed. Temperature measurements with fMRI could define the region of inactivation to a resolution of 1.25 mm, far higher than any other method. However, the cyroloop used in previous studies cannot be directly applied to fMRI experiments for one major reason. The cyroloop is made out of steel. Steel tubing cannot be used in fMRI studies because of the ferromagnetic properties of steel. However, there are other plastics like teflon that can be made into tubing with the desired dimensions.

It will also be necessary to design a multiple phase array surface coil. A phase array surface coil is a combination of individual surface coils. The advantage of a multiple phased-array surface coil as opposed to a single coil, which covers the same area, is that the phased-array coil has a higher Signal-to-Noise Ratio (SNR) [8]. Finally, it is necessary to develop a method or use an existing method to measure the temperature distribution in the brain with fMRI to accurately define the region of inactivation. A resolution of ~2 mm^3 and uncertainty of ±1 ^{o}C would be sufficient. Temperature measurements using MRI-technology have been done before, and a similar methodology may be used in this situation with some minor variations [9-11]. This thesis presents the solutions to the problems described above.

§2 OBJECTIVES

This thesis presents the solutions to a number of problems directly related to using reversible inactivation by cooling in conjunction with awake monkey fMRI experiments. These solutions will make it possible for neuroscientists to obtain more information about the functional impact of anatomical connections between various regions of the brain. Specifically, this includes:

(1) Designing a cooling system and coolant probe capable of reversibly cooling a region of interest (ROI) on the surface of the cortex. The cooling probe when placed immediately above the tissue should not alter the image and should be capable of cooling the tissue from 37 ^{o}C down to ~ 20 ^{o}C.
(2) Develop or adapt an existing method to measure the temperature distribution with MRI in the monkey brain with a resolution of ~ 1.25 x 1.25 x 1 mm^3 and precision of ±1 ^{o}C. It would also be desirable if the method could be easily incorporated into the fMRI sequence.

(3) The design and construction of a receive coil (phase array) that will be used to measure the temperature distribution in the brain and can obtain functional images (gradient-echo echo planar images (GE-EPI)).

The following sections present the detailed solution to the problems described above. I begin first with the design of the cooling system.

§3 COOLING SYSTEM DESIGN

This section describes the various parts in the cooling system. First, I will describe the general components of the cooling system (i.e. pump, tubing, fluid, etc.), and then I will discuss the coolant probe separately.

3.1 General Components

The cooling system is quite a simple setup. A schematic of it is shown in Figure 3.1.

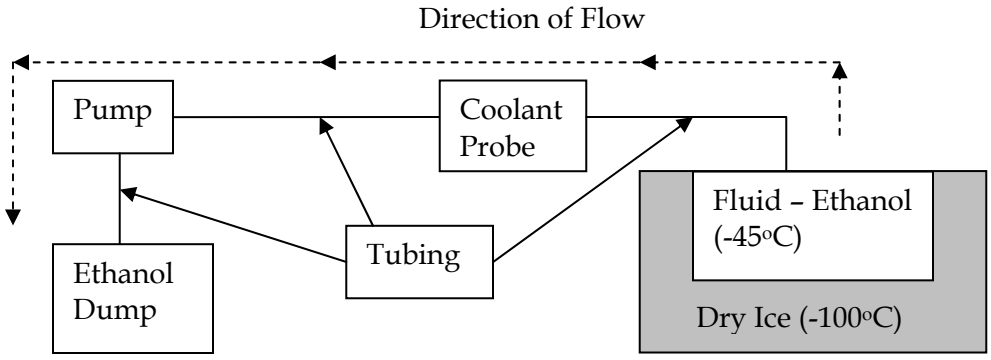

FIGURE 3.1 – SCHEMATIC OF COOLING SYSTEM

The coolant probe will be described in detail in the next section. Below is a list of the rest of the parts in Figure 3.1 and a description of each of them.

TABLE 3.1 – DESCRIPTION OF COOLING SYSTEM COMPONENTS

Part	Description	Company
Pump	QSY - 120 V AC Pump; Flow Rate = 0 – 51.8 mL/min	FMI Pump
Tubing	3 mm OD/2mm ID Teflon Tubing	Upchurch Scientific
Ferrules & Nuts*	10/32″ Thread	Upchurch Scientific
Ethanol	100% Pure Ethanol in 1000 mL Glass Beaker	Aaper Chemical
Dry Ice	CO_2 at ~ -100°C	MGH
Ethanol Dump	1 Gallon Bucket	Rubbermaid

*Ferrules and nuts are not shown in Figure 3.1. A picture of one set is shown in the Appendix Figure A.10. They are used to connect the tubing to the pump and to the coolant probe.

All of the components above were bought and thus did not present much of a challenge to put together. However, the coolant probe is the most important part of the system and was made in-house.

3.2 Coolant Probe

A number of different materials were tried for the coolant probe. The material has to satisfy the following conditions:

(1) Retains ductility at low temperature (-40 ^{o}C).
(2) Strong material that will not break easily.
(3) Be constructed into most any shape.
(4) Should not cause any image artifacts due to its magnetic susceptibility properties.
(5) Biocompatibility

The selection of a material was based on practical considerations along with those above. It would be ideal to find a material that can be easily ordered and not depend on special manufacturing processes. Six different materials were tested. Most materials were some form of polyethylene although a few were glass.

Initially, it was thought a small 'cryoloop' could be created with small tubing (OD ~ 0.6 mm) similar to what was done in the past [1]. The region which needs to be cooled is nearly 1 cm^2. The difficulty with a cryoloop is the fact that it needs to be used in a magnet. Therefore, we can use only magnet-compatible materials. The only material from which tubing can be made that mimics a cryoloop is Teflon. Teflon tubing, however, develops kinks when bent and restricting flow and thus cannot cool. Also, Teflon tubing causes several susceptibility artifacts. Other magnet compatible materials may be constructed into tubing with the aid of special manufacturing process. This option was not explored because of financial considerations and it would take longer to produce.

A more convenient solution compared to a cryoloop, which uses small tubing, is a 'cryosurface'. Instead of having to bend small tubing in the shape of a circle, a disk can be made very thin (~ 0.6 mm) that is in contact with the surface of the brain. With the help of a simple milling machine, these can be constructed into almost any shape (i.e. square, rectangular, etc.). An important drawback of a cryosurface is that it can only be applied to the cortical surface (gyri). It cannot be inserted into other regions deeper in the brain, like the sulci, because of its geometry. For these regions, it will be necessary to alter the cryosurface to fit the folds of the monkey brain. Though the first-generation cryosurface is limited in the regions it can cool, it is sufficient for the initial studies.

An ideal choice for the material of the cryosurface is fiberglass (Polymer Plastics Corp - G10/FR4 Fiberglass – Sheet Thickness 0.05 mm and 0.20 mm). It is quite often used in MRI experiments and does not cause any distortion of the image. A coolant probe of this design turns out to be very convenient for experimental purposes. It does not have to be implanted in the monkey brain, but can be inserted during the experiment and removed after.

A coolant probe was designed in such a manner and proved extremely successful. It is capable of cooling water from at room temperature (~ 20 ^{o}C) to -10 ^{o}C in five minutes. A picture of the coolant probe is shown in Figure 3.2.

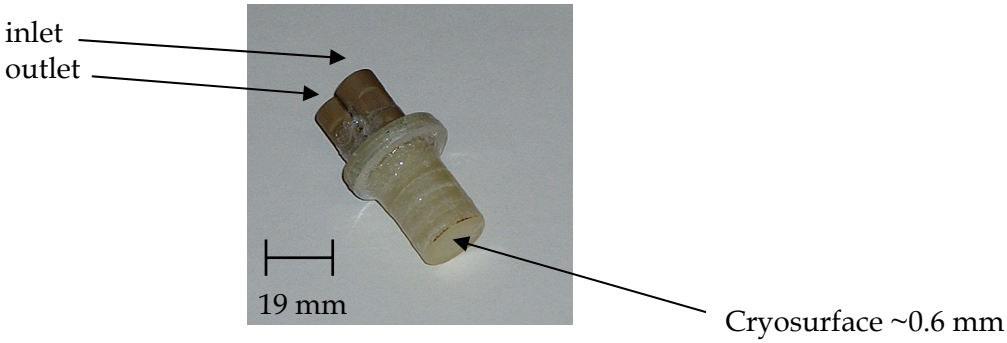

FIGURE 3.2 – PICTURE OF COOLANT PROBE. NOTICE THE INLET AND OUTLET ADAPTERS ON TOP OF THE PROBE.

The coolant probe is glued together using adhesive hardener and resin (Gougeon Corp. - G5 Adhesive Hardener and Resin). The cryosurface is ~ 0.6 mm thick. The coolant probe gets very cold (< -10 ^{o}C) when the ethanol is flowing through it yet it maintains its structural integrity.

The coolant probe will be mounted on the brain of the monkey using the equipment shown in Figure 3.3.

FIGURE 3.3 – (A) HEAD POST FIXTURE A (B) HEAD POST FIXTURE B, AND (C) HEAD POST FIXTURE B MOUNTED ON TOP OF HEAD POST FIXTURE A. HEAD POST FIXTURE A IS SECURED TO THE SKULL WITH DENTAL ACRYLIC AND IS NOT REMOVABLE. THE COOLANT PROBE REMAINS IN HEAD POST FIXTURE B AS TO MAINTAIN A CONSTANT POSITION OVER THE DURATION OF THE STUDY. HEAD POST FIXTURE B IS FIXED TO HEAD POST FIXTURE A DURING THE ACTUAL EXPERIMENT.

Head Post Fixture A is secured to the skull of the monkey using dental acrylic. The coolant probe is placed in Head Post Fixture B to maintain a constant position of the coolant probe during multiple experiments. Head Post Fixture B along with the coolant probe would be removed after the experiment and sterilized for the next use. Figure 3.4 shows the desired configuration of the three pieces (Coolant Probe, Head Post Fixture A, Head Post Fixture B).

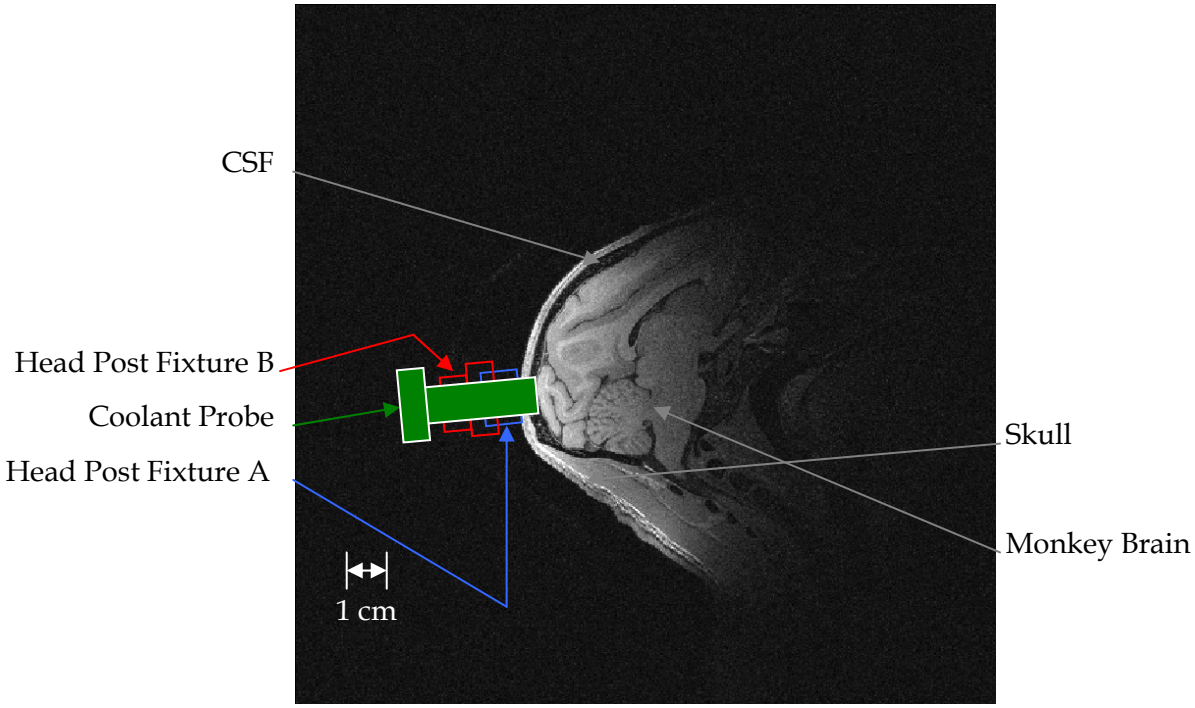

FIGURE 3.4 – POSSIBLE ARRANGEMENT OF COOLANT PROBE, HEAD POST FIXTURE A, AND HEAD POST FIXTURE B ON THE MONKEY SKULL AND BRAIN

The cooling system described in this section meets the first four requirements. It is not possible to address the biocompatibility issues until the material is actually inserted into the brain. The biocompatibility of fiberglass will be tested in the near future when it will be possible to insert the coolant probe into the brain. The next sections focus on how to measure temperature (on-line) with fMRI so that the effect of the cooling system can be quantified during an fMRI experiment.

§4 TEMPERATURE MEASUREMENTS USING FMRI

In order to measure temperature with fMRI, a very well established method called Proton Resonance Frequency Shift (PRF Shift) was used. The method exploits the temperature dependence of the phase of the frequency of ^{1}H. The method is quite precise with uncertainties ranging from ± 0.05 ^{o}C to 1 ^{o}C depending on the sequence parameters of the MRI scan such as the voxel size, TE, and TR.

Thermal maps can be constructed from phase differences images obtained from simple gradient echo sequences [9-11]. This a very well established and robust method. The model of the phase shift sensitivity ($\Delta\phi / \Delta T$) is given by the equation

$$\frac{\Delta\phi}{\Delta T} = \alpha \cdot \omega_o \cdot 2\pi \cdot TE \quad \text{[rad]} \tag{4.1}$$

where: $\Delta\phi$ = phase change in radians
ΔT = temperature change in Celsius
α = thermal coefficient ~ 0.01 ppm/^{o}C
ω_o = Larmor frequency of the magnet
TE = excitation time used in gradient echo sequence in seconds

The parameter α, varies with material. Despite this fact, it only ranges from -0.008 ppm/^{o}C to -0.011 ppm/^{o}C. For our purposes, we will use a value of -0.01 ppm/^{o}C.

The phase is a necessary component to recreate the image so every MRI sequence uses phase information. Thus, for our purposes, it is needed that we save the raw phase data. The phase data is not usual stored with the functional images in conventional experiments. Using MATLAB, the phase data can be read from the scanned file and application of equation (4.1) will provide the temperature distribution for the image. It would be desirable to use the same sequence for temperature measurements and fMRI so that we do not have to acquire two scans. Again, this can be done easily with most fMRI sequences by simply storing the phase data the scanner uses to reconstruct the signal intensity image.

Section 5 describes an experiment in which the temperature distribution in a piece of steak was measured while the cooling system was placed on the surface of the steak. A steak was used because it has a good deal of water in it but can be considered a solid material. Before the experiment is presented, it is helpful to visualize what equation (4.1) is calculating. Figure 4.1 shows the phase image of a piece of steak at the beginning of a cooling experiment. The data were obtained from an EPI sequence taken with a TE of 20 ms, and a TR of 5.0 s. The resolution was 3.1 x 3.1 x 2 mm^3. The figure shows the phase is a random quantity. In other words, its initial distribution cannot be predicted.

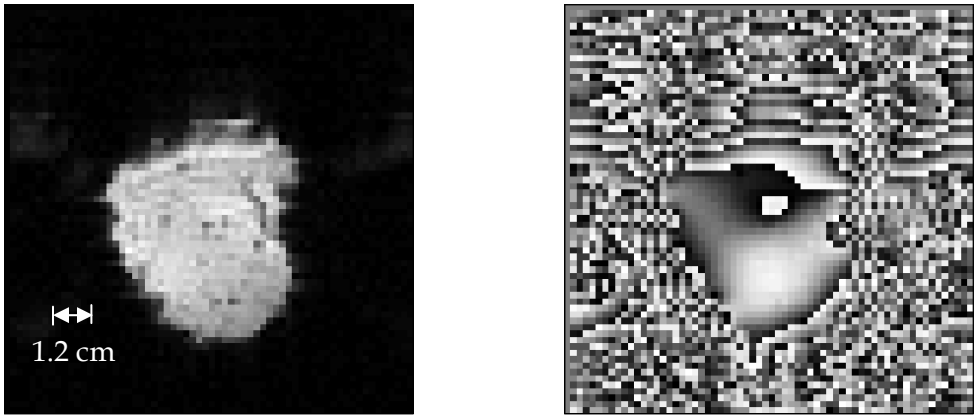

FIGURE 4.1 – (LEFT) SIGNAL INTENSITY IMAGE (RIGHT) PHASE IMAGE OF A PIECE OF STEAK AT THE BEGINNING OF COOLING EXPERIMENT FOV = 200 X 200 MM^2

As the steak is cooled, the phase changes slightly. Figure 4.2 shows the phase image after 10 minutes of cooling. Notice the phase image has gotten brighter in some spots and darker in others.

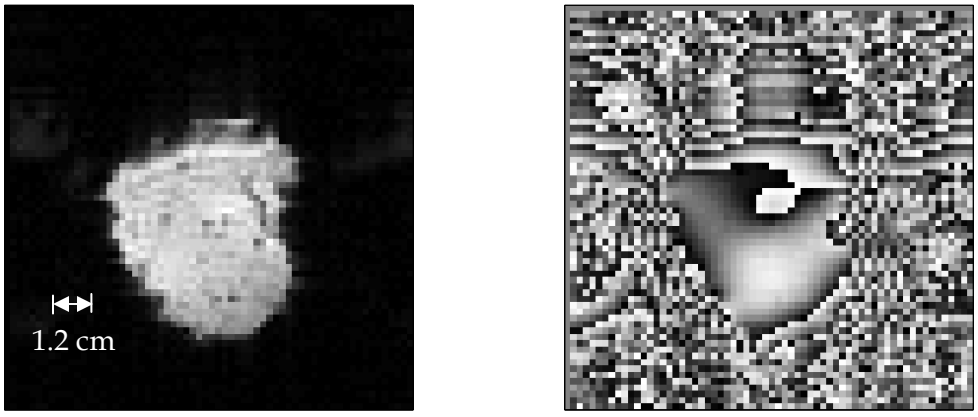

FIGURE 4.2 – (LEFT) SIGNAL INTENSITY IMAGE (RIGHT) PHASE IMAGE OF A PIECE OF STEAK AFTER 10 MINUTES OF COOLING.

Even though the phase data change with temperature, the signal intensity image does not change. This is an important fact since fMRI is based on the signal intensity of the image. If it were to change appreciably, the most important data would be lost. To show this, the signal intensity image from Figure 4.1 was taken at t = 0 s, and it was compared with a image taken at t = 5 s. Data were not calculated in the black region (i.e. low signal intensity) shown in the analysis. The standard deviation of the signal was ± 2.32 %. In other words, on average, the signal intensity varied ± 2.32 % when the scans were taken 5 seconds apart. The data from Figure 4.1 were then compared with the data from Figure 4.2 which were obtained ten minutes later. The standard deviation of the percent difference in signal intensity was ± 2.38 %. Thus, the variation in the signal intensity is constant over the first ten minutes of the experiment. The variance did not increase after 10 minutes either. The same analysis was performed on just the coolant probe region to make sure there is not larger fluctuation in this critical area. The natural fluctuation was ± 1.45% and the fluctuation in signal intensity after 10 minutes was ± 1.46%. Since individual fMRI sequences take place over a maximum of 5 minutes, there will be no effect on the signal intensity of the image from cooling.

The regions in the phase images above where the contrast turns from bright white to completely black correspond to the regions when the phase changes from 2π to 0. This presents a slight problem in the analysis of the data. The scanner stores the phase data in a range from -4096 to 4096, representing values from 2π to 0. When the data are analyzed, the jump from 0 to 2π must be taken into account and adjusted. For example if the phase changed from 1.9π to 0.1π, simple application of equation (4.1) would give a $\Delta\phi$ = -1.8π whereas it should be 0.2π. Equation (5.1) predicts the maximum phase change for a sequence with a TE = 20 ms, ω_o = 128 MHz (corresponds to a 3 T scanner), ΔT = -25 °C to be

$$\Delta\phi = -\alpha \cdot TE \cdot \omega_o \cdot \Delta T \cdot 2\pi = -0.01 \cdot 0.02 \cdot 128 \cdot 25 \cdot 2\pi = 4.02 \ \text{[rad]} \qquad (4.2)$$

Since it is known the temperature is only getting cooler in the steak (in this case), the phase change can only be negative. A phase change from 0.1π to 1.9π, (-1.8π) would correspond to a temperature increase of nearly 40 °C. Thus, we can say that for any temperature change > -0.5π (to allow for slight increases in temperature in regions far away from cooling) we take

$$\Delta\phi_{jump} = \Delta\phi - 2\pi \tag{4.3}$$

This properly adjusts for the jump from 0 to 2π as equation (4.3) gives the correct result of 0.2π. A Matlab code was written to analyze the data from this experiment and correctly adjust for the discontinuity of the phase range (see Appendix). The relative temperature distribution (ΔT) is shown below for the two images shown in Figure 4.1 and 4.2.

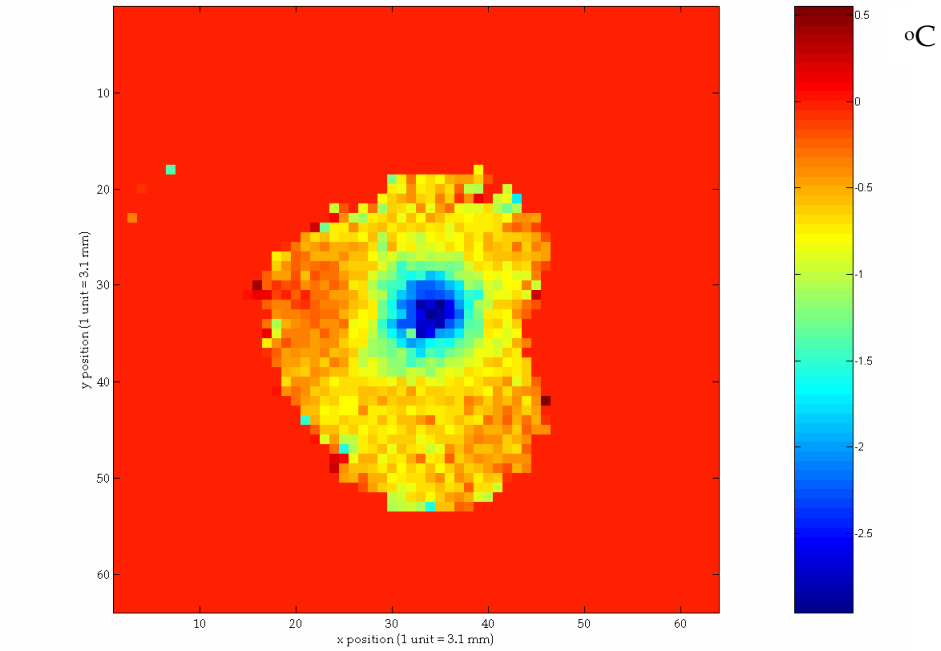

FIGURE 4.3 – 2D DELTA TEMPERATURE (ΔT) DISTRIBUTION (°C) OF A PIECE OF STEAK AFTER 10 MINUTES OF COOLING.

The next section describes in detail the experiment that was performed to test the coolant system and the accuracy and precision of the PRF shift method.

§5 TEMPERATURE MEASUREMENTS OF COOLING SYSTEM

Once the cooling system had been developed along with the general ability to measure temperature with NMR, it was necessary to put the two aspects of research together. This will be the closest approximation to the real experiment with an awake monkey. In these experiments, the accuracy and precision of the temperature measurements are quantified. The experiments took place in Bay 3 at the NMR Center at the Charlestown campus of Massachusetts General Hospital on June 10th, 2003 and June 20th, 2003.

5.1 First Experiment

The first experiment took place on June 10th, 2003. The data from this experiment was not used to quantify the accuracy and the precision of the method but showed a number of important factors involved in using PRF Shift to measure temperature.

5.1.1 Purpose

The purpose of this experiment was to measure the temperature of a piece of steak at various times using a 3 Tesla MRI scanner. The steak was cooled by the coolant probe shown in Figure 3.2. The coolant probe had ethanol flowing through it at ~ –45°C and in the second half of the experiment, water was used at 3 °C instead of ethanol. In the first experiment, the steak was cooled with the ethanol and the thermocouples were inserted in three separate locations. In the second part of the experiment, the steak was cooled with water and then allowed to warm up again in a short time. For this case, only the temperature at the center was measured.

5.1.2 Materials

A number of materials were needed for this experiment (see list below). Below is list of them. The Appendix (Figures A.5-A.10) shows pictures of the setup, which might be helpful for visualization purposes.

(1) Steak
(2) Dry Ice
(3) Large Cooler
(4) One large beaker (~ 3000 mL) (for ethanol)
(5) Pump
(6) Tubing
(7) Coolant Probe
(8) Styrofoam container (for steak)
(9) Styrofoam Sheet
(10) Luxtron® Fluoroptic Thermocouple (Accuracy ± 0.1 °C)
(11) Luxtron® Fluoroptic Thermocouple Extensions
(12) Luxtron® 3100 Fluoroptic Thermometer
(13) 3 Tesla Scanner

5.1.3 Procedure

(1) Logged into the scanner.
(2) Placed the steak in the Styrofoam container into the magnet.
(3) Placed the coolant probe onto the steak.
(4) Taped the tubing of the coolant probe to the Styrofoam box.
(5) Placed the cooler (with dry ice and beaker filled with ethanol in it).
(6) Placed the inlet tube in to the large beaker and placed the outlet tube into the ethanol container.

(7) Placed the thermocouples in the desired position on the steak. Attached the thermocouple extensions to them and connected them to the measurement device.
(8) Secured all connections in the coolant system.
(9) Took a scout scan on the scanner to make sure the steak was in the proper position.
(10) Took a EPI scan of a slice of the steak and made sure the steak was in the proper orientation for the sequence parameters.

TABLE 5.1 – SEQUENCE PARAMETERS FOR EPI SEQUENCE USED IN MEASUREMENTS

Name	TE [ms]	Voxel Size [mm]	FOV [mm]	Bandwidth [Hz]	Time [s]	Slices [ ]	# Scans [ ]
epi_2d_bold_hij	20	3.1 x 3.1 x 2	200	3500	25	1	5

(11) Turned on the pump with the cold ethanol and scanned for 20 minutes. Recorded the temperature in 30 second intervals (data in Appendix).

TABLE 5.2 – SEQUENCE PARAMETERS FOR EPI SEQUENCE USED IN MEASUREMENTS

Name	TE [ms]	Voxel Size [mm]	FOV [mm]	Bandwidth [Hz]	Time [s]	Slices [ ]	# Scans [ ]
epi_2d_bold_hij	20	3.1 x 3.1 x 2	200	3500	1200	1	240

(12) Turned on the pump with the cold water and scan for 1 hour. Recorded the temperature in 30 second intervals (data in Appendix).

TABLE 5.3 – SEQUENCE PARAMETERS FOR EPI SEQUENCE USED IN MEASUREMENTS

Name	TE [ms]	Voxel Size [mm]	FOV [mm]	Bandwidth [Hz]	Time [s]	Slices [ ]	# Scans [ ]
epi_2d_bold_hij	20	3.1 x 3.1 x 2	200	3500	3600	1	720

(13) Cleaned up the entire Bay and then transferred the data to the personal computer.

5.1.4 Results and Analysis

It should be noted that in this section the measured temperature corresponds to data obtained from the thermocouples and calculated temperature corresponds to the data obtained from the phase images. All images are 200 mm by 200mm.

The data taken in step (11) were critical because they attempt show how accurate the PRF shift method is for a large temperature change. In this case, the coolant probe cooled the steak from 14.5 ^{o}C to -5.5 ^{o}C within nine minutes. The probe was frozen to the steak at the end of the measurement.

The data were analyzed with the computer program shown in the Appendix. A sample temperature distribution is shown below along with the position of the thermocouples and where the data were taken from.

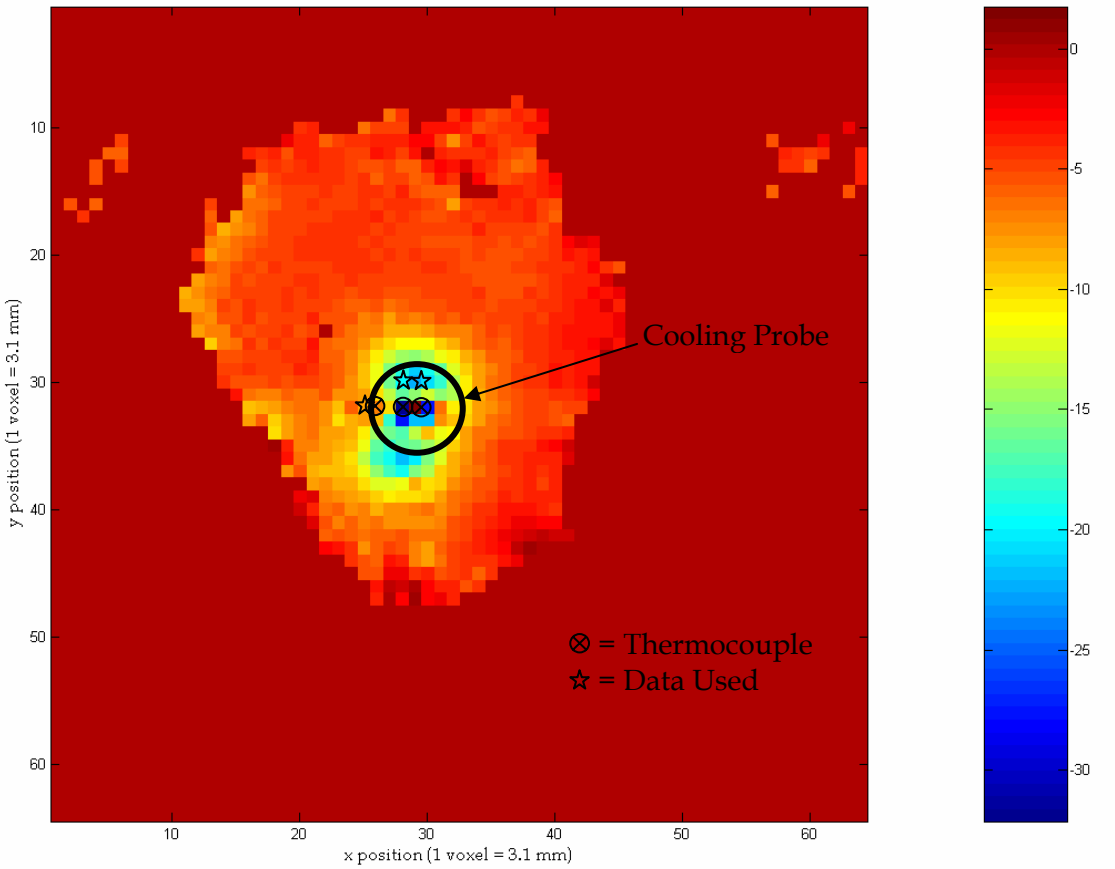

FIGURE 5.1 – 2D DELTA TEMPERATURE (ΔT) DISTRIBUTION AFTER 10 MINUTES OF COOLING WITH ETHANOL. THE FIGURE SHOWS THE LOCATIONS OF THERMOCOUPLES AND DATA USED. NOTICE THAT THE TEMPERATURE DISTRIBUTION IS NOT SYMMETRIC. THIS IS DUE TO THE FACT THAT THE SLICE WAS TAKEN SLIGHTLY TO CLOSE TO THE COOLANT PROBE AND THE STEAK WAS FROZEN IN THE CENTER. HOWEVER, THE DATA AROUND THE ROI IS NOT AFFECTED.

The slice taken in the figure above was taken too close to the coolant probe and so the entire image is not solely of a piece of steak. More importantly, the region under the coolant probe is frozen. In general, MRI images are not as accurate when the water molecules are frozen since MR imaging is based on the resonance of hydrogen in the liquid form of the water molecule. These two factors cause the image under the coolant probe to be inaccurate. However, the data from the points surrounding the thermocouples were near the coldest region and provided some measure of the temperature in this region. These points can be expected to be lower than the measured values since the measured values were taken at the coldest part of the steak (the center). The data from the specified points in Figure 5.1 were taken every 30 seconds and compared with the thermocouple data. Each scan was five seconds long and so the scan from 25 - 30 seconds was averaged with the scan from 30 – 35 seconds for a single time point. Figure 5.2 compares the calculated temperature values to the measured values at the three locations

over the time of the experiment.

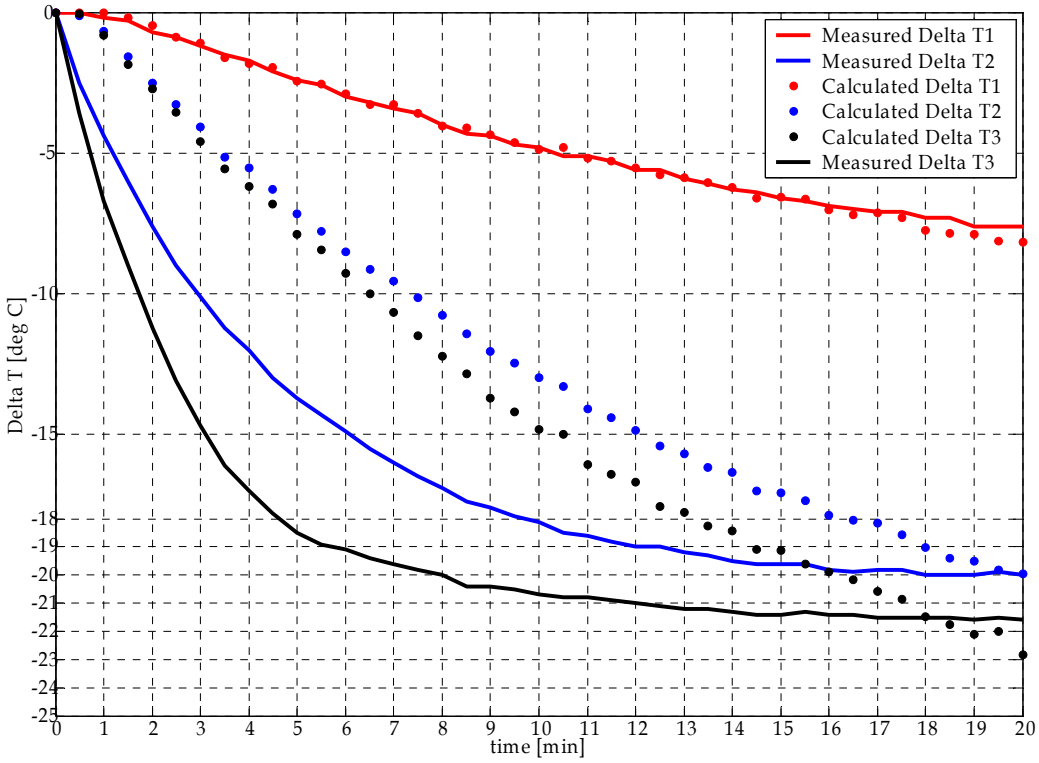

FIGURE 5.2 – CALCULATED AND MEASURED DELTA T VS. TIME AT THREE SPECIFIED POINTS IN STEAK. IN THE REGION RIGHT BELOW THE COOLANT PROBE, THE CALCULATED TEMPERATURE DOES NOT RESPOND QUICKLY TO THE TEMPERATURE GRADIENT. IN THE REGION OUTSIDE THE COOLING PROBE WHERE THE TEMPERATURE CHANGES SLOWLY, THE CALCULATED VALUES EXACTLY FOLLOWS THE MEASURED VALUES.

The calculated temperature values obtained from the phase data of the scan do not change as quickly as the measured values for the data points in the center of the probe. There are two reasons why calculated temperature does not follow the measured temperature curve. First, the points used in the analysis are not in the exact location of the thermocouples and are closer to the edge of the coolant probe which is clearly a warmer region. Second, after 3 minutes, the steak was frozen in the region under the coolant probe. Thus, the data from this region are not reliable and another experiment must be performed to correctly quantify the accuracy of the PRF Shift method at the center of the probe.

In the region where the temperature steak is not frozen, the calculated values exactly follow the measured values. Every point is within ± 0.4 ^{o}C of the measured value. The image quality in this region was not affected since the steak was not near the freezing point.

This part of the experiment shows that the method can accurately measuring a slowly varying temperature distribution. A second experiment must be conducted to quantify the accuracy of the method in regions of fast temperature changes. In the second part of this experiment,

chilled water was used instead of ethanol, in order to cool the steak only moderately and then the pump was shut off and the steak was allowed to warm up again. The experiment lasted over an hour. The data obtained after 40 minutes were not accurate because the phase drifts began to show non-linear behavior. The first order method used to adjust for the phase described below is not applicable in this circumstance.

The figure below compares the thermocouple data with the measured temperature values over the first 40 minutes of the experiment.

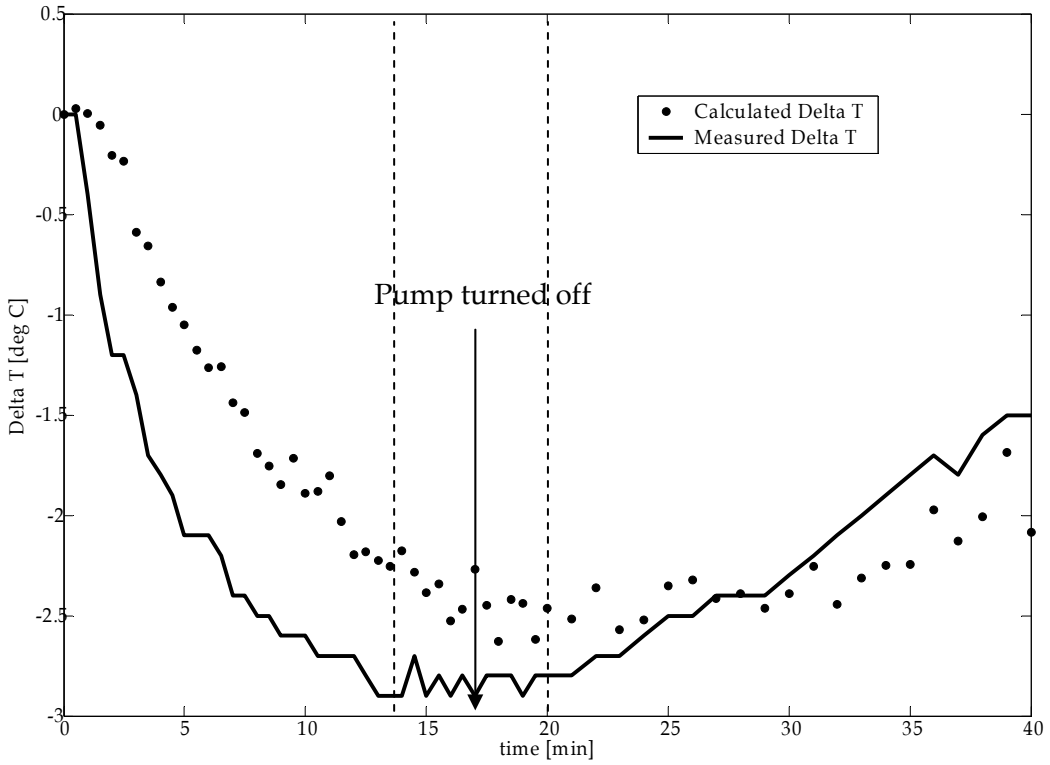

FIGURE 5.3 – ADJUSTED DELTA TEMPERATURE (ΔT) VS. TIME AT CENTER POINT IN STEAK. AGAIN WE SEE THE CALCULATED TEMPERATURE IS ACCURATE WHEN THE DISTIRBUTION STABLIZES AND SLOWLY FOLLOWS THE TEMPERATURE WHEN IT IS CHANGING. THE DASHED LINES REPRESENT THE REGION IN WHICH THE TEMPERATURE POINT UNDER CONSIDERATION IS NOT CHANGING.

Again, we see the same pattern as in Figure 5.2. When the temperature is changing, the calculated data are not as accurate as when the distribution is in steady state. The data between the dashed lines in Figure 5.3 were averaged. The measured value with the thermocouple was -2.8 ^{o}C and the averaged calculated value was -2.5 ^{o}C. The accuracy is in the range of ± 0.6 ^{o}C .

It should be noted that the data in Figure 5.3 was adjusted for phase drift. The phase drift in this experiment was quite large. A set of four data points far away from the coolant probe was used to adjust the data. The set of four points is denoted in Figure 5.5. Figure 5.4 shows the phase drift in the region. The temperature was known not to change appreciably in this region due to the fact that the temperature measured two voxels above these points did not change by more than -0.7 ^{o}C.

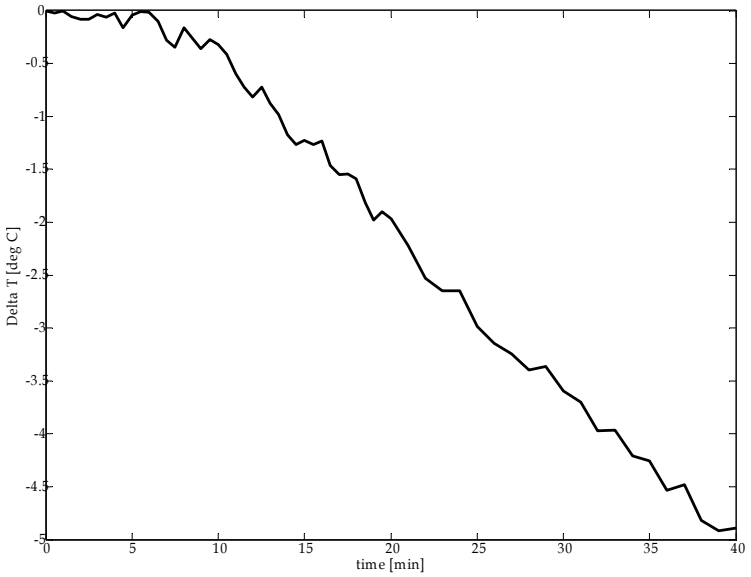

FIGURE 5.4 – PHASE DRIFT IN UNITS OF DELTA TEMPERATURE (ΔT) IN °C VS. TIME FOR THE SET OF FOUR DATA POINTS. THE TEMPERATURE OF THE FOUR DATA POINTS DID NOT CHANGE BY MORE THAN -0.7 °C ACCORDING TO A THERMOCOUPLE IN THE REGION.

The phase drift in this particular experiment was rather large. The phase drift continues to grow after the 40 minutes shown here. The first order adjustment used for the first 40 minutes does not give good results after 40 minutes. It is not known why the drift is so large and it is necessary to study this phenomenon more carefully in the future. The data in Figure 5.3 was adjusted by simply subtracting the data in Figure 5.4. The slice was taken further below (2 mm) the coolant probe and it shows the appropriate temperature distribution. Figure 5.5 shows a sample delta temperature distribution 15 minutes after cooling.

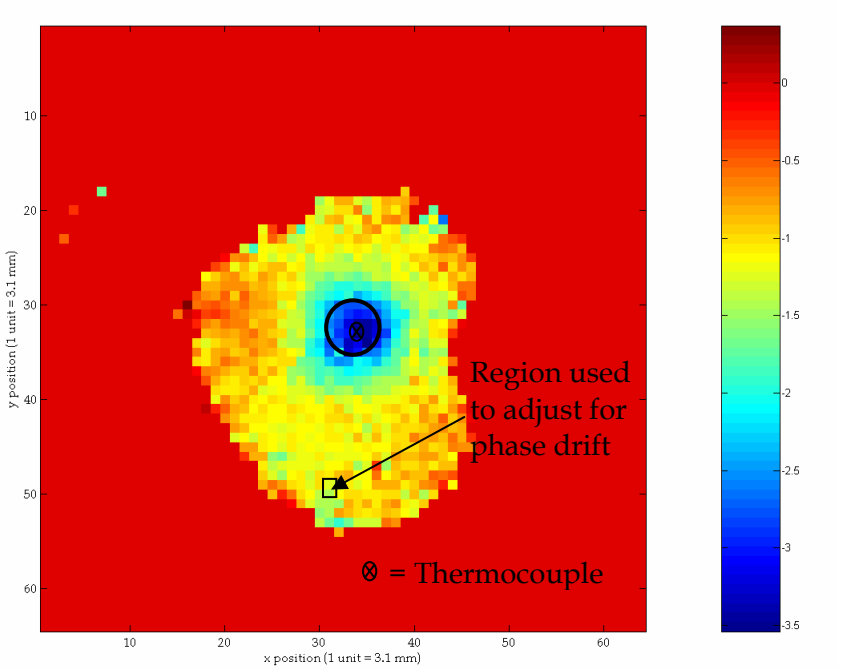

FIGURE 5.5 – 2D DELTA TEMPERATURE DISTRIBUTION (ΔT) IN °C AFTER 15 MINUTES OF COOLING. THE DATA WAS TAKEN FROM THE EXACT LOCATION OF THE THERMOCOUPLE.

A much better slice of the object was taken in this experiment. The temperature distribution is symmetric immediately below the coolant probe. It can be said that the PRF shift method is quite accurate when a slowly varying temperature distribution is present (< 0.2 °C/min). In this region, the calculated data was accurate to ≤ ± 0.6 °C . The uncertainty in the temperature measurements was a constant value of nearly ± 0.07 °C in each experiment. The uncertainty was calculated by taking the standard deviation of the two images used to in calculating a single temperature point. It should be noted that the experiments were carried out using a resolution of 3.1 x 3.1 x 2.0 mm^3 voxel dimensions.

The first experiment showed the expected symmetric temperature distribution could be measured with PRF Shift, and quantified the accuracy of the method for regions of slow temperature change. However, a second experiment was required to quantify the accuracy of the PRF Shift method in the center of the probe were there is the greatest temperature change. In the second experiment, phase drift was taken into account, there was more than one slice, and the resolution was 2.1 x 2.1 x 1.0 mm^3.

5.2 Second Experiment

The purpose of the second experiment was to quantify the accuracy of the PRF Shift method in the center of the probe were there is the greatest temperature change.

5.2.1 Improvements

The materials and the procedure for the second experiment were the same as the first experiment with the following improvements:

(1) A small piece of the steak was cut off and placed next to the main piece of steak which was being cooled. The small piece of steak was used to correct for phase drift since it was known that the temperature of this piece did not change throughout the experiment.
(2) The EPI sequence was altered to take 7 slices of the steak (1 every 2 mm) and the resolution of the sequence was increased from 3.1 x 3.1 x 2.0 mm^3 to 2.1 x 2.1 x 1.0 mm^3.
(3) A large temperature gradient was created in the center of the steak, but the steak was not allowed to freeze and thus the image quality at maximum cooling was not sacrificed.

5.2.2 Results and Analysis

Two sets of data were acquired in this experiment. In both cases, the cryosurface of the coolant probe did not sit level on the steak resulting in a slightly asymmetric temperature distribution. The FOV in this experiment was 135 mm x 135 mm for all images. During the acquisition of the first data set, the thermocouple came loose and all the measured temperature data was lost. However, Figure 5.6 shows the temperature distribution for all seven slices at the time when the steak was being cooled.

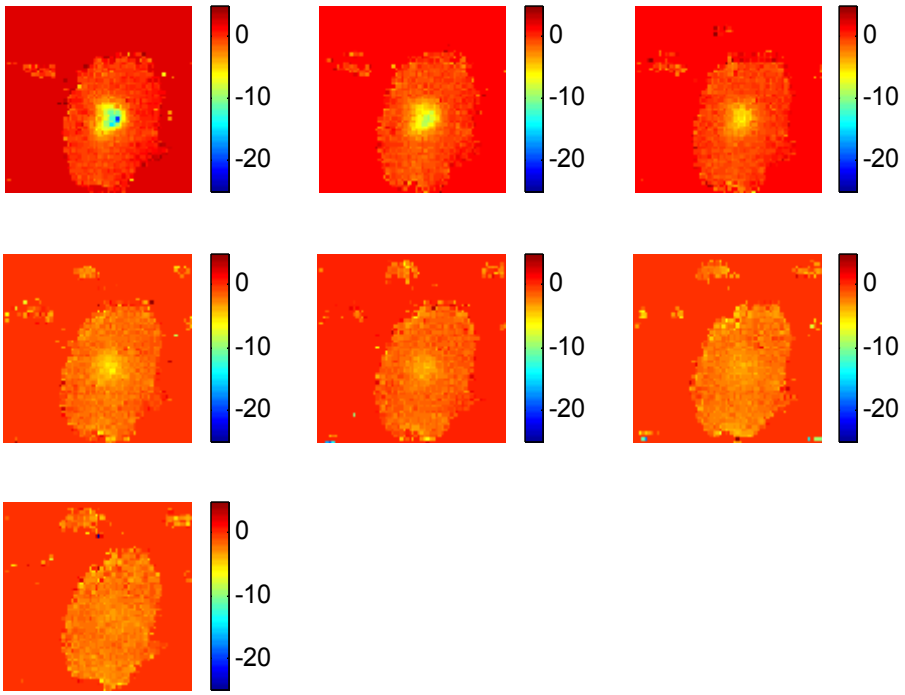

FIGURE 5.6 – MULTISLICE TEMPERATURE DISTRIBUTION IN °C DURING COOLING. THE FIRST IMAGE IS CLOSEST TO THE COOLANT PROBE. NOTICE HOW ALL THE SUBSEQUENT IMAGES SHOW A SMALLER TEMPERATURE CHANGE. EACH SLICE WAS 1 MM THICK AND THE SLICES WERE 2 MM APART.

During the acquisition of the second data set, the thermocouple did not move and so a comparison between the measured data and the calculated data could be made at the center of the probe. Figure 5.7 shows an image of the slice closest to the probe and the relative locations of the thermocouple.

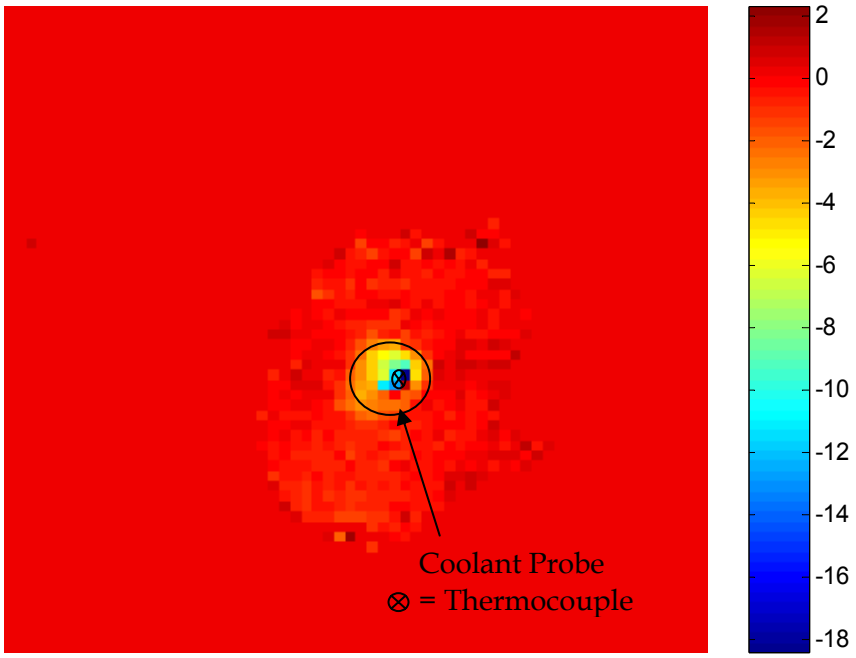

FIGURE 5.7 – 2D TEMPERATURE DISTRIBUTION IN °C OF SLICE CLOSEST TO COOLANT PROBE. THE IMAGE SHOWS THE RELATIVE LOCATIONS OF THE COOLANT PROBE AND THE THERMOCOUPLE.

Ideally, the four data points surrounding the thermocouple would have been used to calculate the average temperature in the region surrounding it. However, the data point in the lower right hand corner was at a fat boundary and all phase information was lost.

A small piece of steak was placed next to the cooled steak. The small piece of steak remained at a steady temperature throughout the experiment and thus provided a measured of phase drift. The small piece of steak can be faintly seen in the image shown in Figure 5.8.

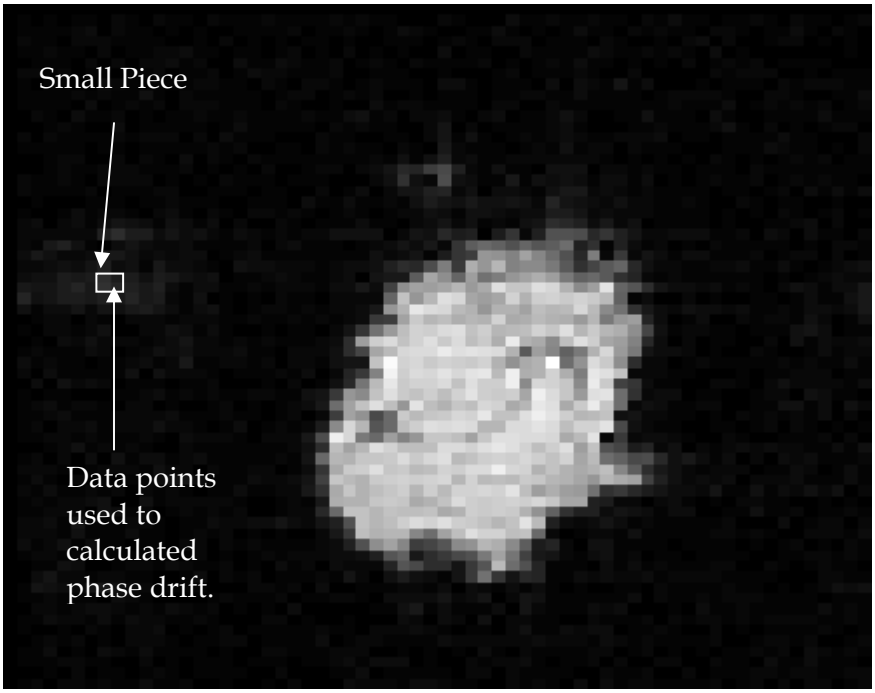

FIGURE 5.8 – SIGNAL IMAGE OF STEAK SHOWING THE LOCATION OF THE SMALL STEAK USED TO ADJUST FOR PHASE DRIFT. THE FIGURE SHOWS THE FOUR POINTS USED TO ADJUST THE TEMPERATURE DATA.

The experiment took place over 13 minutes so there was little phase drift. Figure 5.9 shows the phase drift used to adjust the temperature of the image over time. The data from Figure 5.9 was calculated by taking four points next to each other in the middle of the small piece.

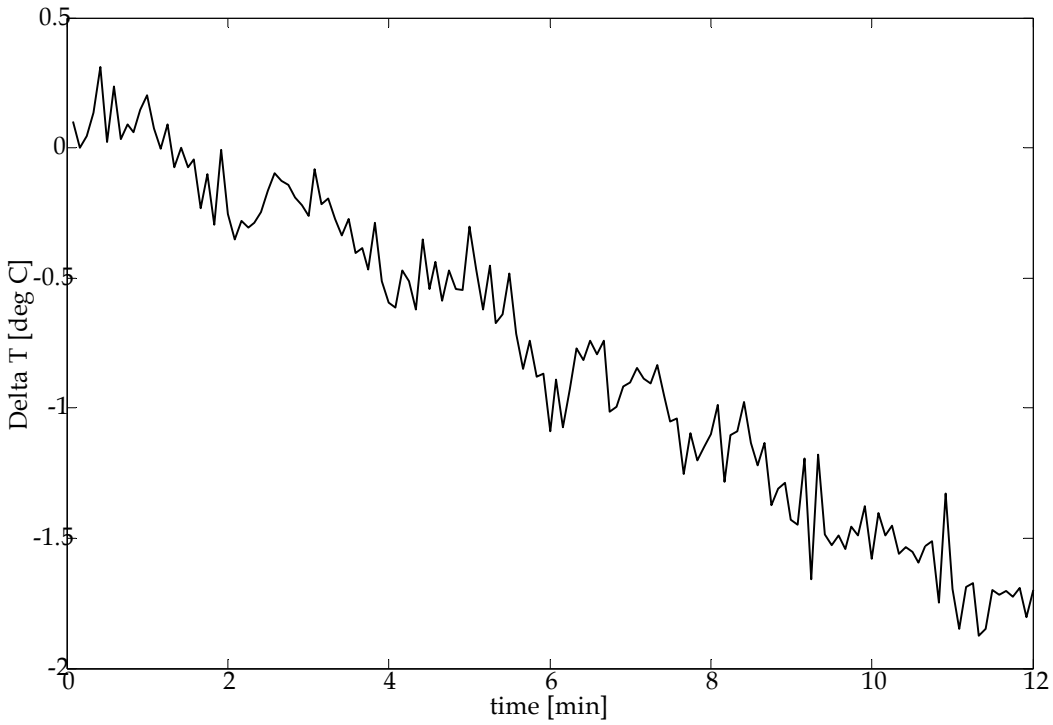

FIGURE 5.9 – PHASE DRIFT VS. TIME FOR FOUR POINTS USED TO ADJUST TEMPERATURE DATA. THE EXPERIMENT TOOK PLACE OVER 13 MINUTES SO THERE WAS NOT MUCH PHASE DRIFT.

The phase drift in this experiment is 1.8 ^{o}C after 12 minutes compared to 1.4 ^{o}C in the previous experiment. The raw temperature data was adjusted by subtracting the phase drift. The measured data can be compared to the calculated data. Figure 5.10 shows the results.

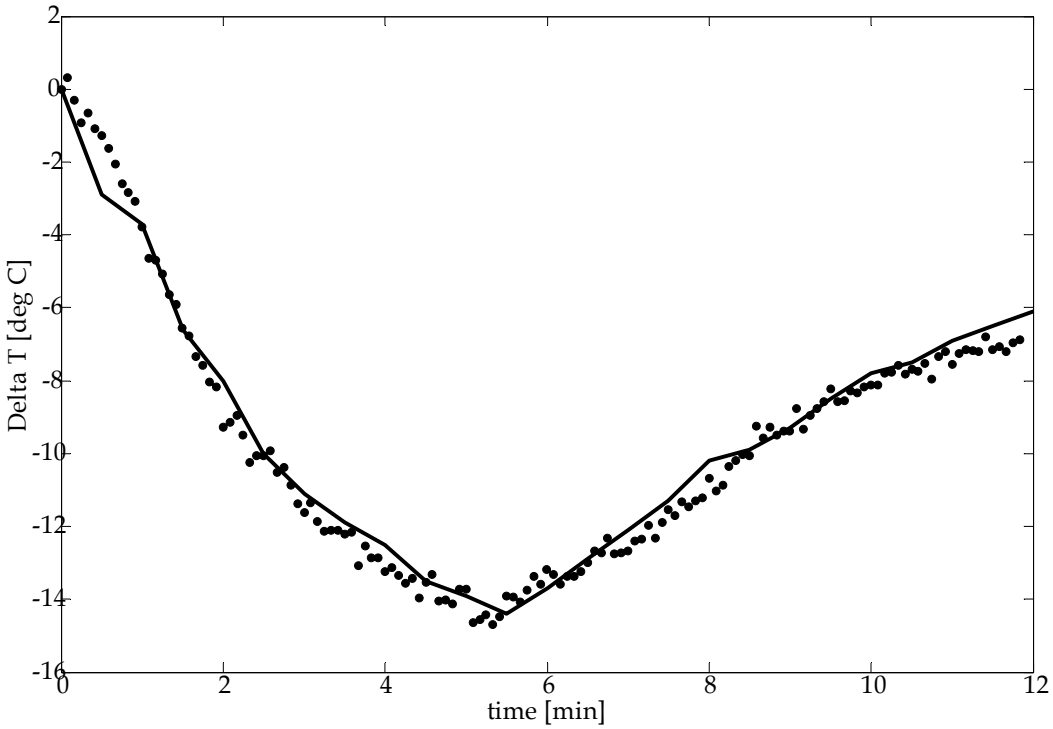

FIGURE 5.10 – MEASURED ΔT VS. CALCULATED ΔT IN °C IN THE CENTER OF COOLANT PROBE. THE CALCULATED DATA FOLLOWS THE MEASURED DATA.

The calculated data is within ± 0.6 °C of the measured value throughout the entire experiment. Thus, it can be concluded that the PRF Shift method can accurately measure a time dependent temperature distribution to ± 0.6 °C when the data is adjusted for phase drift. The data can be acquired in multislice format of the desired resolution (~ 4 mm^3). The precision of the measurements in this experiment (uncertainty in the calculated data) was 0.15 °C. The precision in this experiment was worse than the first experiment since the resolution was higher.

§6 HEAD COIL DESIGN

The coils used in the MR-scanner must be able to respond to high frequencies (298.3 MHz, at 7T) in very large magnetic fields where there is stray capacitance surrounding the coil. The design of the coil for this type of system is a bit tedious.

The coil is designed in such a way to minimize the noise contribution. Therefore, instead of having one large head coil, it is more advantageous to build three small ones (termed phase array). This way the signal adds together so the signal intensity is not lost but the noise contribution is minimized. The sections below outline the steps taken to complete such a task. The steps outlined below has been slightly modified from those described by Wald (1995).

6.1 Material Considerations

It would be desirable to choose a material that is not magnetic but has good inductance and electrical conductivity. Also, the material has to be flexible because it will be placed on a plastic mold of the monkey's head which is curved. Strength of the material is also a consideration because the coil should be as robust as possible.

The material used in most instances is a thin non-magnetic plastic-copper composite. It has a thin layer (0.5 mm) of copper on top of a thin layer of plastic (0.5 mm). The copper is used as the conducting material and the plastic is used for strength and stability while maintaining ductility. The total material thickness is no greater than 1 mm. The material is expensive as it costs nearly $200 for two square feet but proves to work best under experimental conditions.

All three coils have been designed and manufactured using this material using the methods described below.

6.2 Circuit Design

In our case, a coil that excites the proton spins in the brain (transmit coil) has already been constructed and is functional. Therefore, it is necessary to construct only a receive coil. The purpose of the receive coil is to receive the reflected signals from the monkey brain after stimulation. These signals resonate at 298.3 MHz ± 0.3 MHz (at 7T). It would therefore be desirable to design a coil such that it only absorbs signals at or around 298.3 MHz. The following sections describe how each individual coil is designed and then how they are coupled together.

6.2.1 Individual Circuit Design

Theoretical considerations suggest that a simple LC circuit will suffice to produce a circuit resonance at 298.3 MHz. This is true to a certain extent and constitutes the main part of the circuit. However, a simple LC circuit alone will not suffice because we have to have some way to turn the circuit on and off (called "tuning" and "detuning" the circuit) so that it does not interfere with the transmit coil and relaxation processes. This leads to a modified LC circuit called a BAL-UN circuit. The term BAL-UN stands for balanced – unbalanced circuit, which refers to the tuning states. A general schematic of the circuit is shown below:

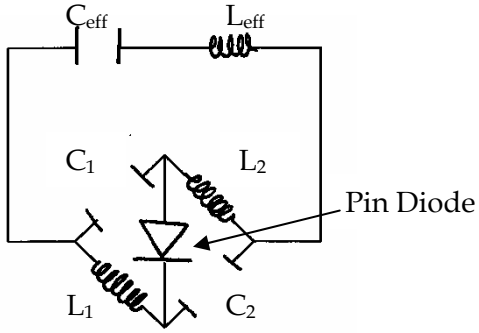

FIGURE 6.1 – GENERAL SCHEMATIC OF CIRCUIT USED FOR RECEIVE COIL

By changing the biasing on the pin diode, we find the frequency response of the coil changes significantly. The figure below shows the effective circuit for both conditions.

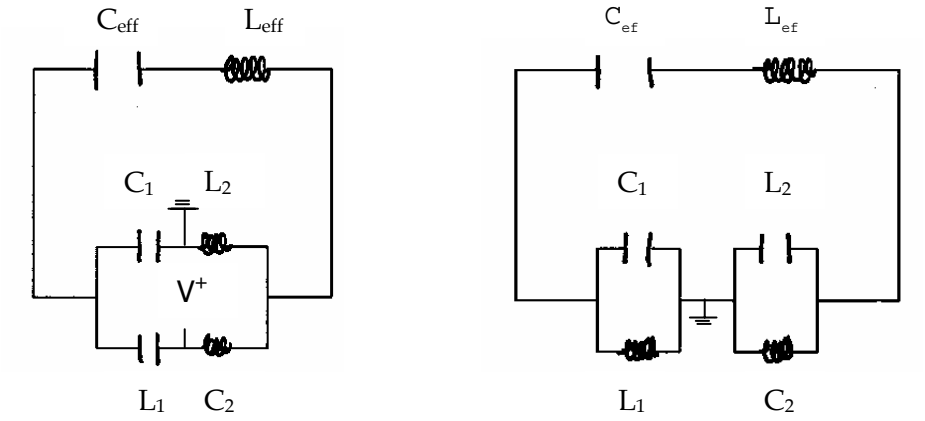

FIGURE 6.2 – EFFECTIVE CIRCUIT AFTER FORWARD/REVERSE BIASING THE DIODE. THE CIRCUIT IS IN RECEIVE MODE WHEN THE DIODE IS REVERSE BIASED.

When the circuit is reverse biased, we would like the circuit to absorb signals at 298.3 MHz = ν_o. Therefore, it is necessary to make the resistance of the circuit zero (in reality the resistance will n ever be zero because of the small resistance in the wire). This can be done easily by choosing:

$$\left.\begin{aligned} z_{C_{eff}} + z_{L_{eff}} &= 0 \\ z_{C_1} + z_{L_2} &= 0 \\ z_{C_2} + z_{L_1} &= 0 \end{aligned}\right\} \; at \;\; \omega = 2\pi\nu_o \tag{6.1}$$

where: z_i = the impedance of the i^{th} particle

Recall that the impedance for a capacitor and inductor are of opposite sign for oscillating signals thus it is possible for their sum to be zero. When it is forward biased, we don't want any signal at 298.3 MHz to be absorbed because the transmit coil is trying to excite the brain with a 298.3 MHz signal. Therefore, we can choose

$$\left.\begin{aligned} \frac{1}{\frac{1}{z_{C_1}} + \frac{1}{z_{L_1}}} = \infty \;\; &\Rightarrow \;\; z_{C_1} + z_{L_1} = 0 \\ \frac{1}{\frac{1}{z_{C_2}} + \frac{1}{z_{L_2}}} = \infty \;\; &\Rightarrow \;\; z_{C_2} + z_{L_2} = 0 \end{aligned}\right\} \; at \;\; \omega = 2\pi\nu_o \tag{6.2}$$

These equations directly imply that

$$\left.\begin{aligned} z_{C_1} &= z_{C_2} \\ z_{L_1} &= z_{L_2} \end{aligned}\right\} \; at \;\; \omega = 2\pi\nu_o \tag{6.3}$$

in addition to the other constraints posed above. The figure below illustrates the effective circuit under the properly chosen parameters as described above for the various bias settings.

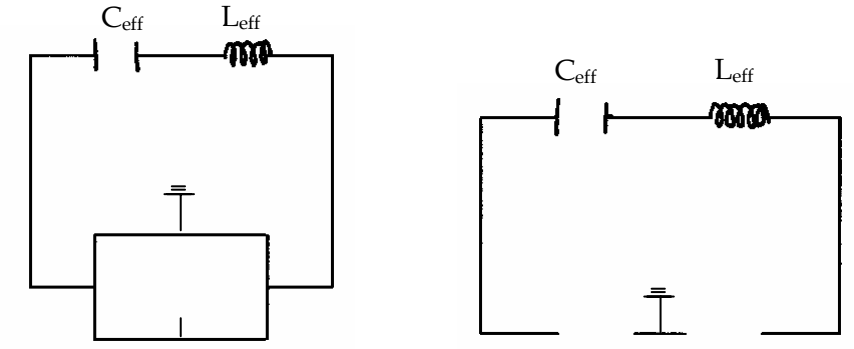

Reverse Biased Forward Biased

FIGURE 6.3 – EFFECTIVE CIRCUIT UNDER FORWARD AND REVERSE BIASING CONDITIONS WITH THE CIRCUIT PARAMETERS CHOSEN AS DESCRIBED BY EQUATIONS (6.1) – (6.3). NOTE THAT WHEN THE CIRCUIT IS FORWARD BIASED IT CANNOT CREATE A SIGNAL BECAUSE IT IS ESSENTIALLY AN OPEN CIRCUIT.

There is no choice for the values of C_{eff} and L_{eff} since L_{eff} is a property of the material (in this case copper). L_{eff} turns out to be ≈ 56 nH. Therefore, C_{eff} ≈ 5 pF. One might ask however, can any values of C_1, C_2 etc. be chosen as long as they satisfy the relations above? The answer to this question is no. Impedance matching must be taken into consideration. Impedance matching assures that the maximum power transfer is obtained when a electronic signal is transmitted between two different lines (in this case the coil to the cable).

The impedance we are referring to in this case is the monkey's head. Since the coil essentially sits on the monkey's head, the monkey's head represents an impedance (i.e. resistance to flow of electrons). Since the circuit is designed to work with high frequency signals, if this impedance is not taken into account during circuit design then the signal received from the object in the coil will not be properly transmitted through the cable. Thus the values of C_1, C_2, L_1, and L_2 must be chosen to account for the impedance of the monkey's head so that proper signal transfer is achieved.

In order to maximize the power transfer through impedance matching, we chose to geometrically average the resistance in the coil with the 50 Ω impedance of the network analyzer. We chose a geometric average due to the nature of the equations representing the

reflection and transmition coefficients of high frequency electronic signals. This results in the constraint on the values C_1 and L_2.

$$\left|z_{matching}\right| = \sqrt{50R} = \left|z_{C_1}\right| = \left|z_{L_2}\right| \; at \; \omega = 2\pi\nu_o \tag{6.4}$$

where: R = resistance of the loop [Ω].

A value of R is picked and then the circuit is constructed until a good response function is found. R was found to be 9 Ω for these coils. This leads to a value of $C_1 = C_2 \approx 27$ pF and $L_2 = L_1 \approx 6$ nH. The effect of loading and unloading is shown in Figure 6.5.

A great deal of trial and error is necessary to find the exact right values. The ideal response function for the forward/reverse biased circuit is in Figure 6.4 under loading:

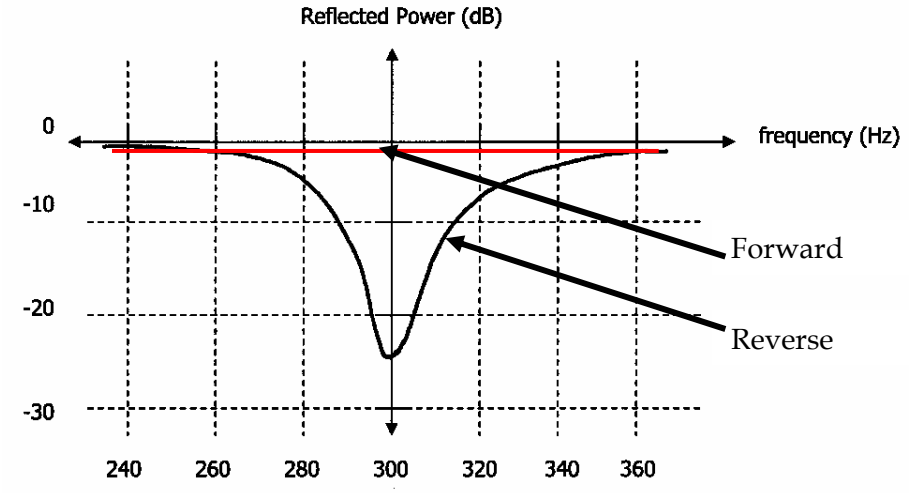

FIGURE 6.4 – IDEAL REFLECTED POWER RESPONSE FUNCTION OF A FORWARD/REVERSED BIASED CIRCUIT UNDER LOADING. NOTICE THE DIP IN REFLECTED POWER AT 298.3 MHZ CORRESPONDING TO THE RESONANCE OF THE CIRCUIT IN THE REVERSED BIASED CASE.

Recall that the equation for decibels is

$$\mathrm{dB} = 10\log_{10}\left(\frac{P_{in}}{P_{out}}\right) \tag{6.5}$$

where: P_{in} = power put into the system
P_{out} = power out of the system

Thus a reflected power value of -20 dB at the resonance frequency implies that the circuit absorbs 99% of the power of a signal at that frequency. The reflected power response function for the forward biased case is very similar to that shown above. In reality, the power response functions don't look exactly as shown above. Some have resonances at other frequencies. The circuits are so small and sensitive to the physical orientation of the capacitors and the loading, the small loop with C_1, L_2, etc. has its own resonance. Therefore, it is quite possible to see

various actual response functions. Also, when the circuit is not loaded, it does not respond as well since it is not impedance matched. Regardless of the extra resonances, there should always be a large resonance at 298.3 MHz.

In order to illustrate the effect of impedance matching consider the figure below. It is the response function for one of the three different coils that I have made when the circuit is reverse biased. Notice the variation in the response function and the difference between a loaded and unloaded circuit.

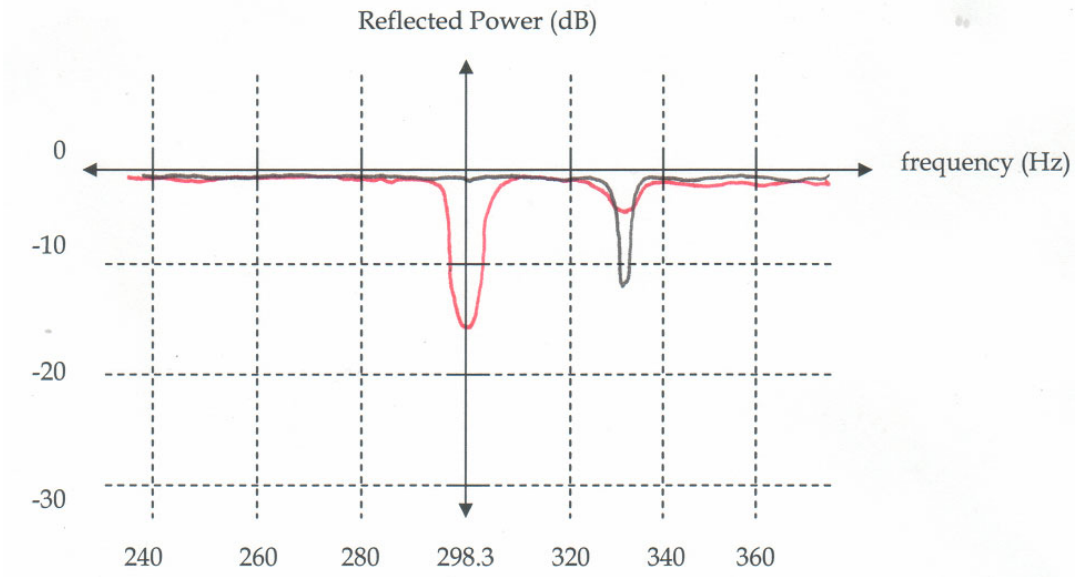

FIGURE 6.5 – REFLECTED POWER RESPONSE FUNCTIONS FOR ONE COIL USED IN HEAD COIL. NOTICE HOW POORLY THE COIL BEHAVES WHEN IT IS UNLOADED SINCE THERE IS NO IMPEDANCE MATCHING (BLACK = UNLOADED; RED = LOADED). SEE APPENDIX (FIGURES A.1 AND A.2) FOR THE TWO OTHER REFLECTED POWER RESPONSE FUNCTIONS.

The peak that is present in most figures is due to the resonance from the inner loop as described above. Now that the three coils have been tested, it is necessary to couple them to the head mold so that they can all work together.

6.2.2 Coupling Effects

The whole purpose of using three separate coils as opposed to one large coil is the advantage we gain in SNR. However, the coils need to cover the same region as a single coil and thus must be put close together. When they are put close together, and since they all have the same resonance frequency (298.3 MHz) they couple to each other. This coupling is unacceptable from an NMR standpoint because the coupling signal will be much larger than the NMR signal. Thus, the coils will not be able to obtain any NMR data. The coils can be decoupled in a rather simple but tedious manner.

The whole concept behind decoupling can be understood from a basic electrodynamics point of view. Recall from electrodynamics that a current traveling in a loop creates a magnetic field as shown below.

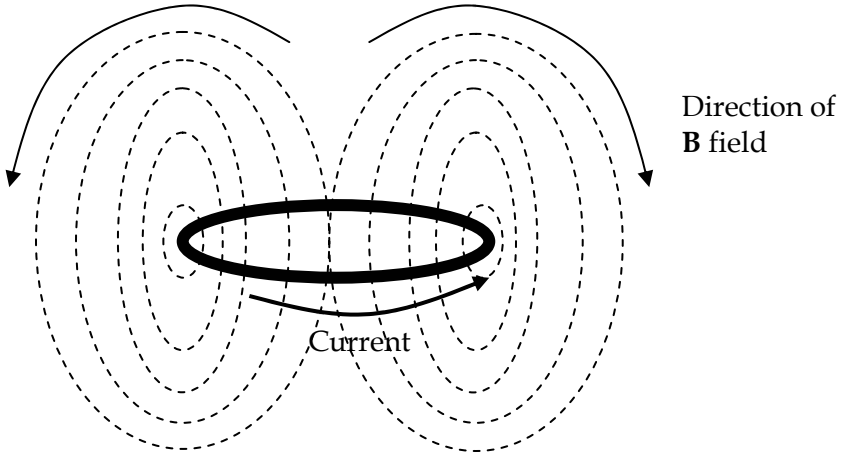

FIGURE 6.6 – MAGNETIC FIELD CREATED BY A CURRENT FLOWING THROUGH A CIRCULAR LOOP

The magnetic field lines are strongest near the coil itself and so if two loops are overlapped as shown in Figure 6.7, then an arrangement can be constructed such that they cancel. This arrangement happens to occur at nearly 1/10 the radius of the loops (assuming they have the same radius). The addition of a third loop requires a similar setup

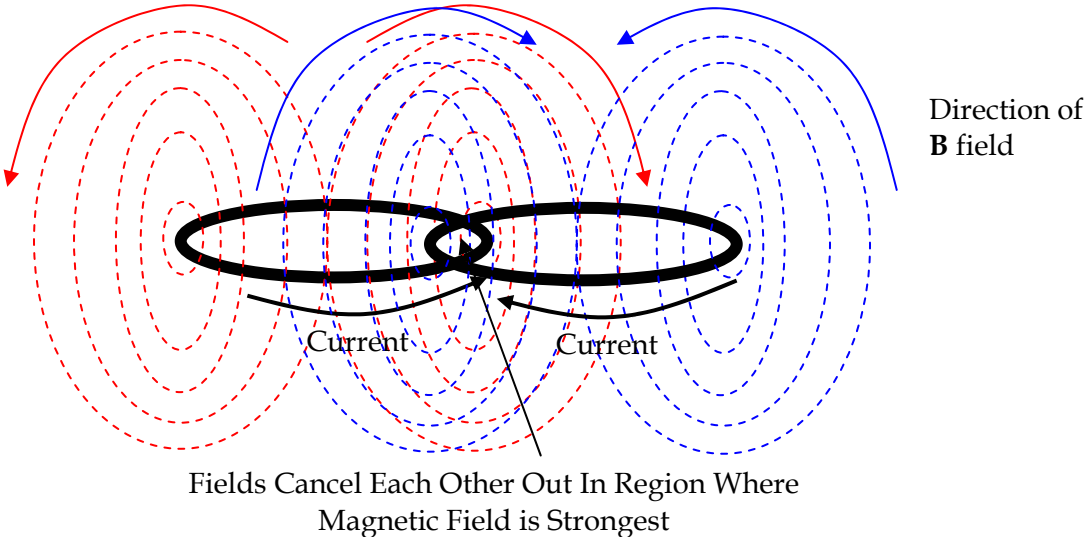

FIGURE 6.7 – POSSIBLE ARRANGEMENT TO CANCEL COIL COUPLING. THE NET MAGNETIC FLUX THROUGH THE LOOPS CANCELS AT NEARLY 1/10 THE RADIUS OF THE LOOPS.

This procedure was done with each of the three coils. In order to test the fact that they are decoupled, the power transfer between each coil was tested. When the loops are near each other and are not decoupled, the power transfer between them is illustrated in Figure 6.8.

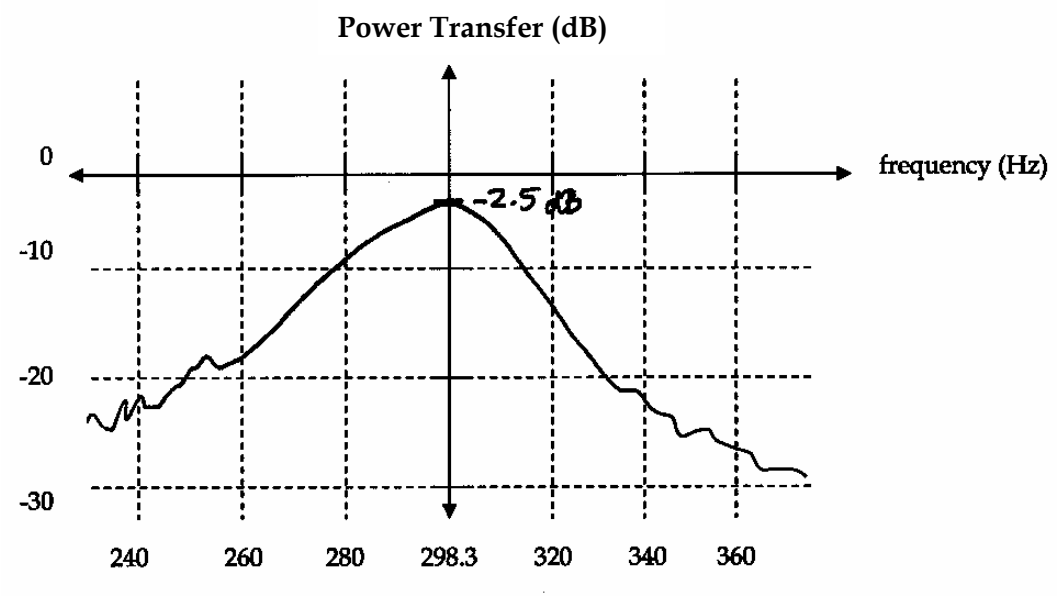

FIGURE 6.8 – TRANSFER POWER FUNCTION BETWEEN TWO COILS WHEN THEY ARE NOT DECOUPLED. -2.5 DB CORRESPONDS TO A POWER TRANSFER OF 56%.

When the coils are placed together in the correct configuration for decoupling, the power transfer function looks like Figure 6.9. This was actually the transfer function between two of our coils. The other power transfer function between the three coils is shown in the Appendix (Figures A.3 and A.4).

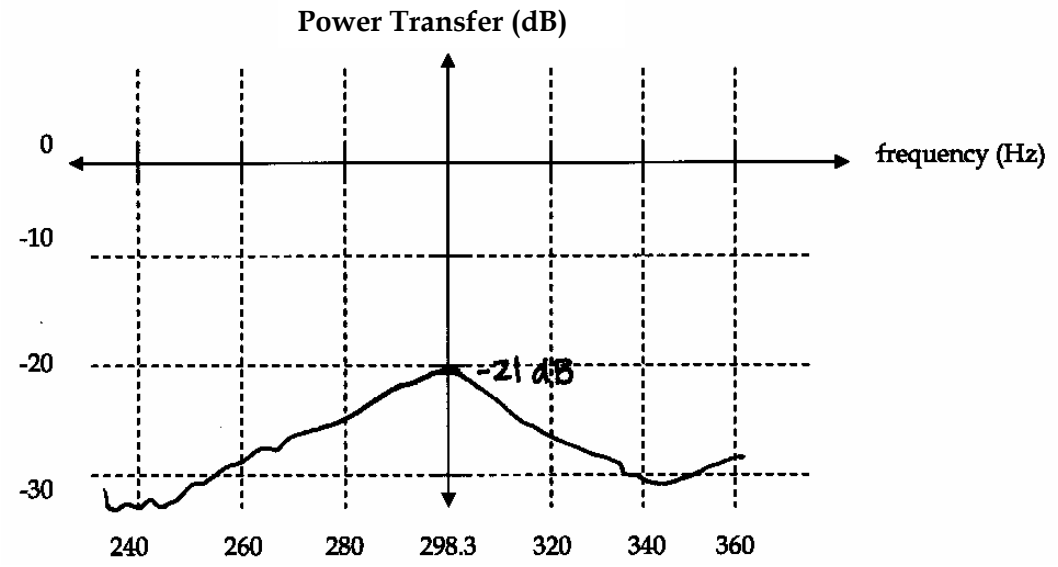

FIGURE 6.9 – POWER TRANSFER FUNCTION BETWEEN TWO COILS WHEN THEY ARE DECOUPLED. -20 DB CORRESPONDS TO A POWER TRANSFER OF 1%.

The coils were mounted on a curved sheet of plastic and glued in placed once the proper configuration was found. Figure 6.10 shows the configuration.

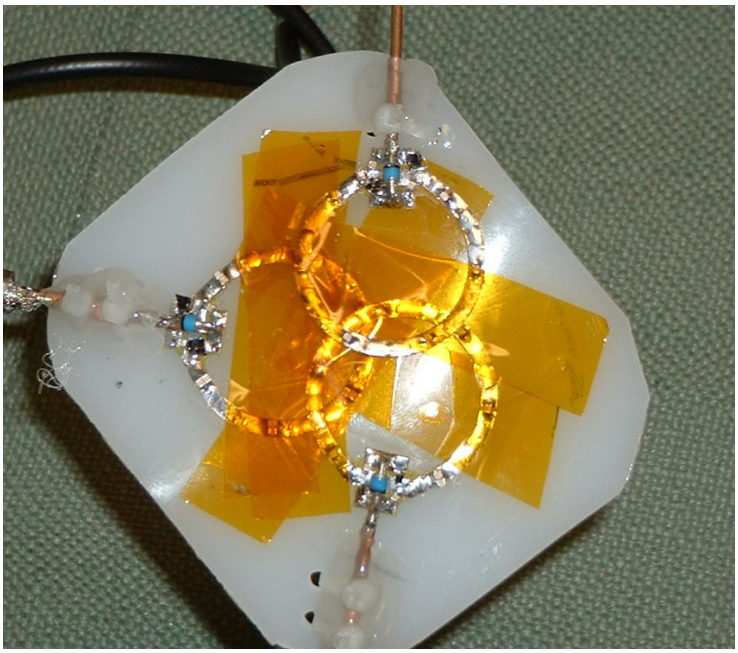

FIGURE 6.10 – PHOTOGRAPH OF FINAL COIL CONFIGURATION

A scan was taken with the MRI machine to finally test if the coils were decoupled. In the test, one coil is activated at a time and the image was analyzed. If the coils are not coupled, then the image will show a bright spot in the center of the coil. If they are coupled, the coils will show an image of each other. The figure below is a test of the three coils.

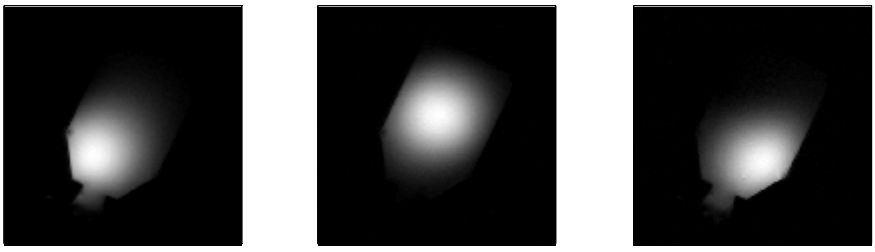

FIGURE 6.11 – MRI SCANNER TEST OF COIL COUPLING. EACH COIL WAS ACTIVATED SEPARATELY. THE THREE IMAGES ARE SHOWN ABOVE. NOTICE IN EACH IMAGE THERE IS NO GHOST OF THE OTHER COILS AS WOULD BE THE CASE IF THE COILS WERE COUPLED.

A simple average of the data shows the FOV of the coils. The image profile is very evenly distributed.

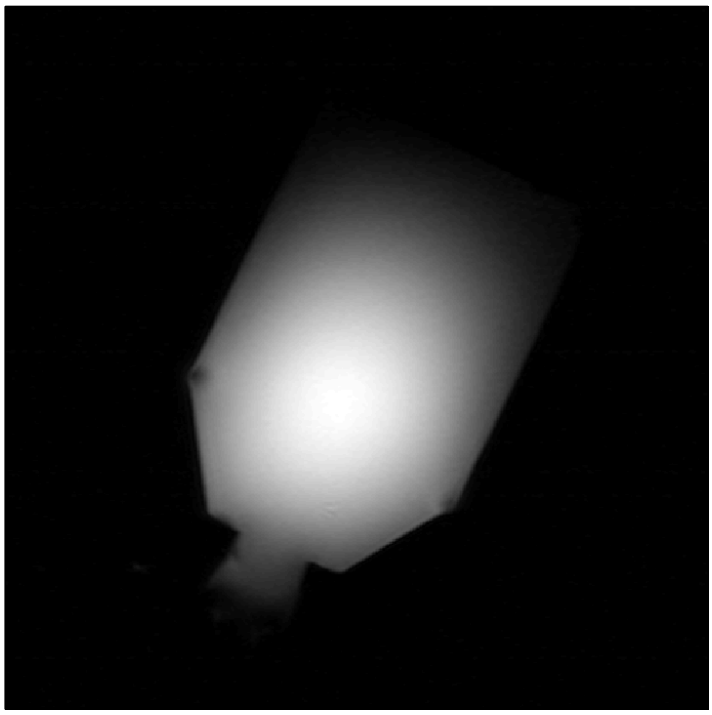

FIGURE 6.12 – SIMPLE AVERAGE OF THE THREE IMAGES FROM FIGURE 6.11. THIS IMAGE SHOWS THE FOV OF THE COIL.

The figure shows that the sum of the individual coils behaves like an individual coil. The imaging properties of the coil was tested in the scanner on May 29th, 2003. The next section describes its performance.

6.3 Imaging Properties

The imaging properties of the coil were tested in the 7T scanner at Massachusetts General Hospital on May 29th, 2003. The coil was placed atop a monkey's head and several scans were taken. The coil performed very well by all standards.

The scanner calculated the signal at a point by taking into account the signal of each of the three coils. The final signal intensity was calculated from the three coils signals using the following equation

$$S_T = \frac{1}{\sqrt{3}}\sqrt{S_1^2 + S_2^2 + S_3^2} \tag{6.6}$$

where: S_T = final signal intensity
S_i = i^{th} signal from the coils

In theory if the noise in each of the coils was not related (i.e. the coils did not measure the same noise), we can calculated the expected improvement in SNR using the error propagation formula below with the following conditions

$$S_T = f\left(S_1, S_2, S_3\right) \tag{6.7}$$

$$\sigma_S = \sigma_{S_1} = \sigma_{S_2} = \sigma_{S_3} \tag{6.8}$$

$$S = S_1 = S_2 = S_3 \tag{6.9}$$

$$\sigma_{S_T} = \sqrt{\left(\frac{\partial f}{\partial S_1}\right)^2 \sigma_{S_1}^2 + \left(\frac{\partial f}{\partial S_2}\right)^2 \sigma_{S_2}^2 + \left(\frac{\partial f}{\partial S_3}\right)^2 \sigma_{S_3}^2} \tag{6.10}$$

where: S = signal from a one coil arrangement
σ_s = noise from a one coil arrangement

The conditions above simply state that all the coils behave the same way and that the signal intensity and noise of the voxel under consideration is the same in each coil. This is not the case for most of the voxels but we are only aiming to get a simple estimate. Inserting the appropriate derivatives we have

$$\sigma_{S_T} = \frac{1}{\sqrt{3}} \sqrt{\frac{S_1^2}{S_1^2 + S_2^2 + S_3^2} \sigma_{S_1}^2 + \frac{S_2^2}{S_1^2 + S_2^2 + S_3^2} \sigma_{S_2}^2 + \frac{S_3^2}{S_1^2 + S_2^2 + S_3^2} \sigma_{S_3}^2} \tag{6.11}$$

which reduces using equations (6.8) and (6.9)

$$\sigma_{S_T} = \frac{\sigma_s}{\sqrt{3}} \tag{6.12}$$

Thus the noise decreases by a factor of $\sqrt{3}$ and so we expect the SNR to be $\sqrt{3}$ higher than an individual coil (~ 170%). As a side note for a general arrangement of N coils, it can be easily shown that

$$\sigma_{S_T} = \frac{\sigma_s}{\sqrt{N}} \tag{6.13}$$

The SNR in the experiment with the three coils was 52 as compared with the single coil which had a SNR of 40. That is a 30% increase. The reason the full 170% is not found is because the noise in each coil is related since they are close to each other. In reality, we cannot use equation (6.10) to calculate the noise improvement for our coil arrangement because the noise in one coil is similar to that in the coil next to it. Regardless, we gain a 130% increase in SNR with the three coil arrangement.

Figure 6.13 shows the image with the three coil array. A comparable image with the same FOV and voxel size was not available with a single coil.

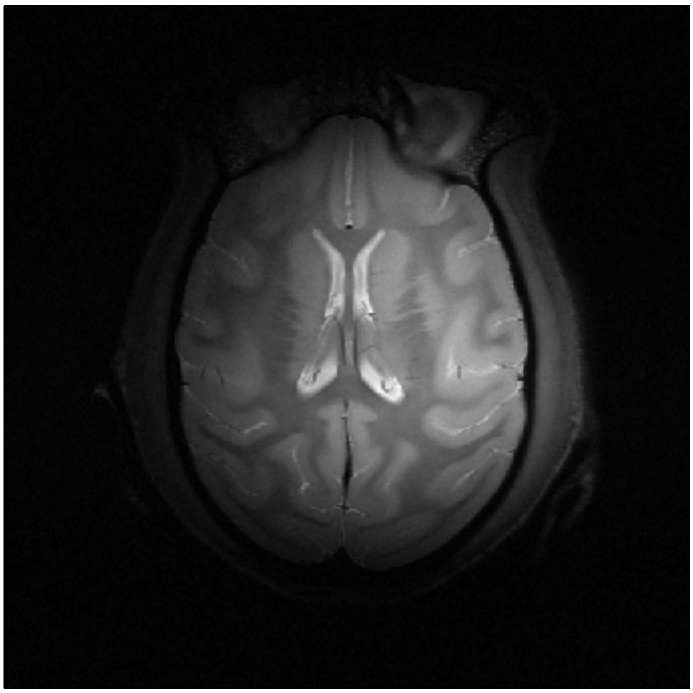

FIGURE 6.13 – IMAGE WITH THREE COIL ARRAY OF MONKEY BRAIN.

The image in Figure 6.13 is satisfactory from a SNR (52) and FOV (~200 mm) perspective.

§7 CONCLUSIONS AND FUTURE WORK

Functional magnetic resonance imaging (fMRI) has been very useful in helping neuroscientists map the brain [1-3]. Functional MRI studies have shown neuroscientists which parts of the visual cortex are activated by various stimuli. Besides knowing which brain areas are involved in the processing of a particular stimulus, or task, it is of great importance to asses the relationship between various neural assemblies. In other words: what kind of calculations are performed in one area and what kind of information is transmitted to the other areas. The method of reversible inactivation is capable of disabling a small region in the brain and looking at the functional consequences of this (reversible) inactivation upon regions anatomically connected to the site [1-3].

A number of problems needed to be solved before reversible cooling could be used in fMRI studies. First of all, it was necessary to design a cooling system that is capable of reversible inactivation and to find a magnet-compatible material that could be placed in the brain (coolant probe) without affecting the image quality. A surface coil needed to be designed with higher SNR. Finally, it was necessary to develop or use an existing method to measure the temperature distribution in the brain with fMRI. A resolution of ~2 mm^3 and uncertainty of ± 1 ^oC is sufficient.

This thesis presents the solutions to these problems. A cooling system and coolant probe were designed with the capability of cooling a piece of steak from room temperature (14.5 ^{o}C) to well below freezing (-5.5 ^{o}C). This cooling capability shows it will be able to cool the monkey brain down to the desired temperature. The cooling system of the probe can cool the brain to a broad range of temperatures by varying the temperature of the fluid (ethanol) and the flow rate.

PRF shift was used to measure the temperature distribution of an object using an fMRI sequence similar to one that will be used in the actual experiment reversible inactivation experiment with an awake monkey. The method was tested and showed accuracy of ± 0.6 ^{o}C compared with thermocouple measurements over 13 minutes for a fluctuating temperature distribution when the data was adjusted for phase drift. The data were taken at a resolution of 2.1 x 2.1 x 1.0 mm^3, and the precision of the measurements was ± 0.15 ^{o}C. The resolution of the measurements was at ~ 4 mm^3 but it can be easily applied at 2 mm^3 only with only a loss in the precision of the measurement.

A phase array head coil was designed with superior imaging qualities to the current single coil. An increase of SNR from 40 to 52 was observed in the image (30% increase) as compared with the calculated increase of 70%. The difference between the observed increase in SNR and the actual SNR is the fact that the coils are close together and measured some of the same noise.

Now that these major obstacles have been overcome, using reversible inactivation in conjunction with fMRI will have many advantages compared to other methodologies [1,6,7]. First of all, now it has been shown that accurate (± 0.6 ^{o}C) temperature distributions can be obtained. This is critical when assessing which regions have been deactivated during the experiment. No other method is capable of having such an accurate temperature distribution in vivo. In addition, the development of a cooling system and magnet compatible coolant probe will allow multiple non-invasive experiments to be performed on a single monkey.

Though the major obstacles to using reversible inactivation along with fMRI experiments have been solved, there is still need for further work in perfecting each aspect of research presented in this paper. Slight modifications can be made to the design of the coolant probe to insure structural stability for all flow ranges. In addition, the head fixture must be implanted in the monkey brain.

Further research has to be conducted on phase drift. It might be possible to adjust the data using phase drift in a different manner to improve the accuracy of our measurements. A second way to improve the accuracy of our temperature measurements is by measuring thermal coefficient, α, which has been shown to depend on the temperature of the heat source and its geometry [12]. By measuring the thermal coefficient, α, of a material similar to brain tissue with the setup used in the fMRI experiments, it might be possible to obtain a value for α more accurate than the value of -0.01 ppm/^{o}C used in this analysis. The thermal coefficient can be measured for such a setup by altering the variables (TE, T, ϕ, etc.) shown in equation (4.1) and extracting α from a linear fit of the data.

Finally, the next generation phase array coil can contain 6-8 coils as opposed to three. This would further increase the SNR ratio and allow higher resolution fMRI/temperature data [8].

REFERENCES

[1] Lomber, Stephen *et al.* "The Cryoloop: An Adaptable Reversible Cooling Deactivation Method For Behavioral or Electrophysiological Assessment of Neural Function", Journal of Neuroscience Methods 1999; 86: 179-194.

[2] Young Investigators Grant, "Interactions Between Areas of the Visual Cortex"; Roeflsema, Pieter; Vanduffel, Wim; Vreeswijk, Van: September 2001.

[3] Lomber SG, Payne BR. "Assesment of Neural Function With Reversible Deactivation Method." Journal of Neuroscience Methods 1999; 86: 105-107.

[4] Vanduffel *et al.* "Functional impact of cerebral connections." PNAS 1997; 94: 7617-7620.

[5] Galuske RA *et al.* "The Role of Feedback In Shaping Neural Representations in Cat Visual Cortex." PNAS; Vol. 99 Iss. 26: 17083-17088.

[6] Malpeli JG. "Reversible Inactivation of Subcortical Sites By Drug Injection." Journal of Neuroscience Methods 1999; 86: 119-128.

[7] Hupé JM *et al.* "Spatial and Temporal Parameters of Cortical Inactivation By GABA." Journal of Neuroscience Methods 1999; 86: 129-143.

[8] Wald L *et al.* "Proton Spectroscopic Imaging of the Human Brain Using Phased Array Detectors." Magnetic Resonance in Medicine 1995; 34: 440-445.

[9] Ishihiara Y, Calderon A, *et. al*. "A precise and fast temperature mapping method using water proton chemical shift. In: Proceedings of the 11th Annual Meeting of SMRM, 1992. pg 4803.

[10] MacFall JR, Prescott DM, *et al.* "MRI Phase Thermometry in-vivo in Canine Brain, Muscle, and Tumor Tissue." Med. Phys. 1996; 23:1775-1782.

[11] DePoorter, J. "Noninvasive MRI Thermometry With the Proton Resonance Frequency Method; Study of Susceptibility Effect." Mag Reson Med 1995; 34: 359-367.

[12] Peters RD *et al.* "Heat Source Orientation and Geometry Dependence in Proton-Resonance Frequency Shift Magnetic Resonance Thermometry." Magnetic Resonance in Medicine 1999; 41: 909-918.

APPENDIX

TABLE OF CONTENTS

Reflected Power Response Functions For Other Two Coils

The figures below are the reflected power response functions for the other two coils.

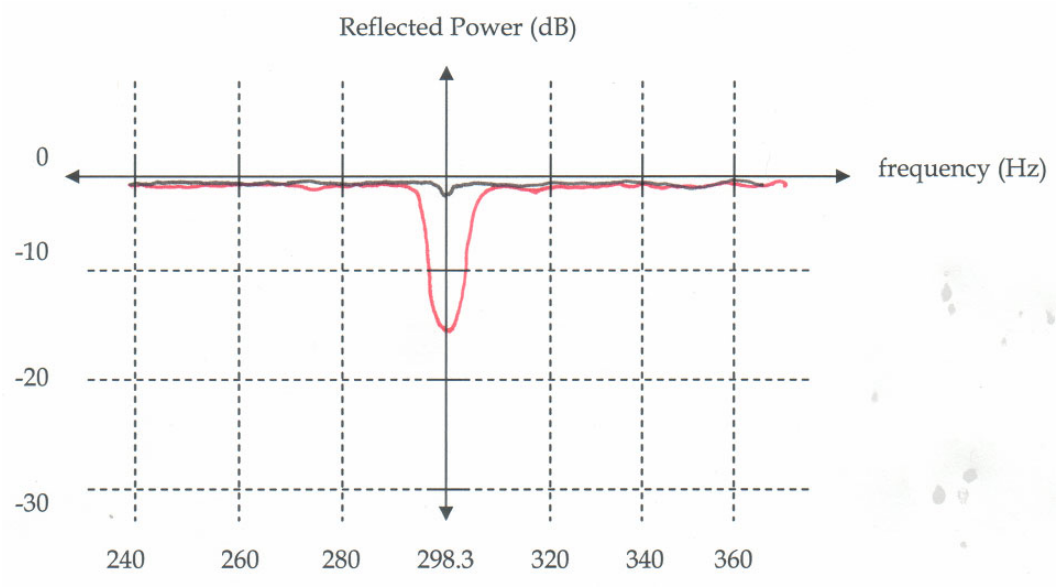

FIGURE A.1 – REFLECTED POWER TRANSFER FUNCTION FOR 2ND COIL

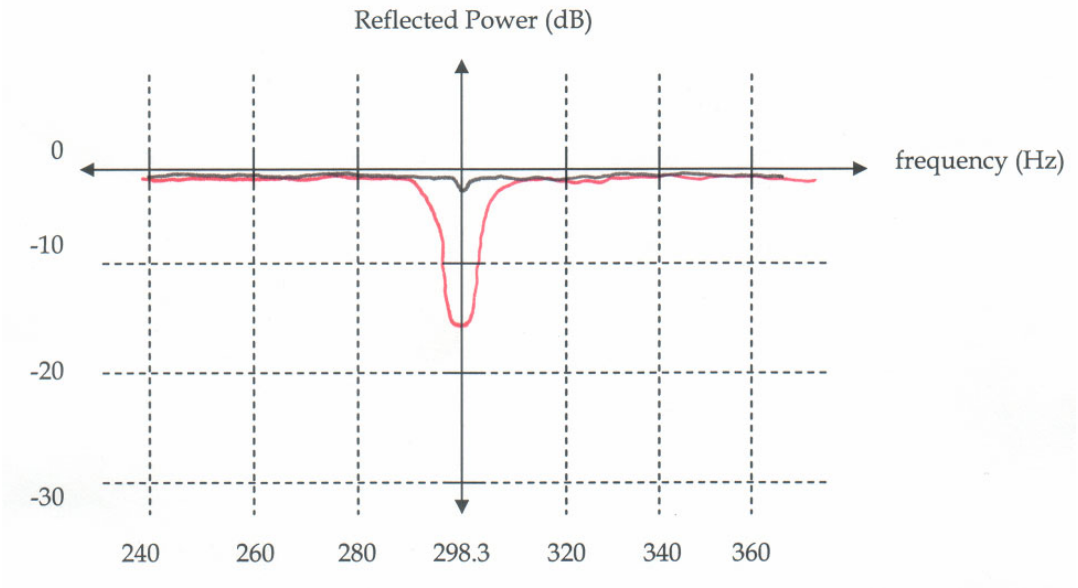

FIGURE A.2 – REFLECTED POWER TRANSFER FUNCTION FOR 3RD COIL

Power Transfer Functions For Other Two Coils

The figures below are the power transfer functions for the other two coils.

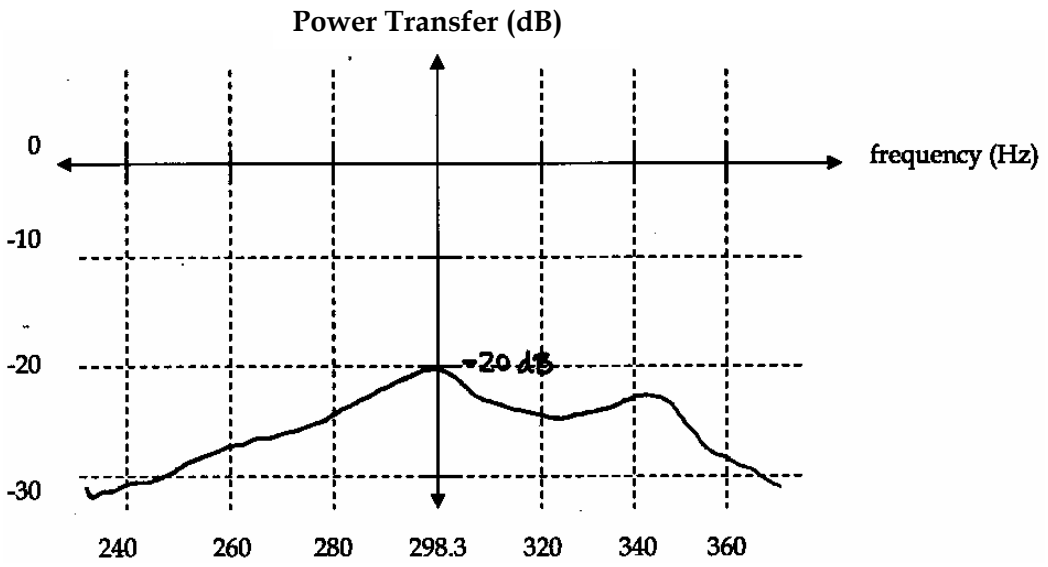

FIGURE A.3 – POWER TRANSFER FUNCTIONS FOR 2ND COIL

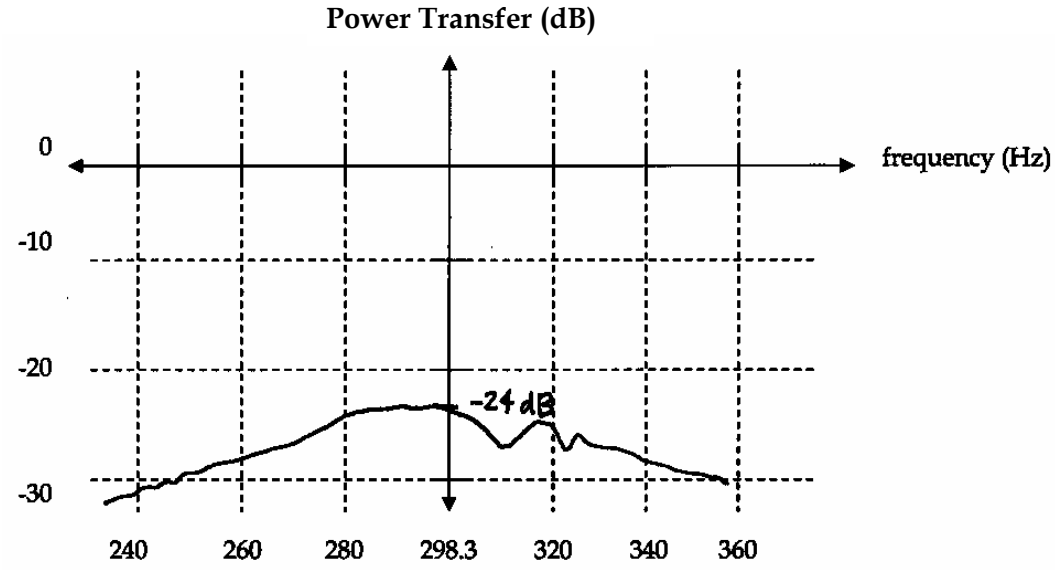

FIGURE A.4 – POWER TRANSFER FUNCTIONS FOR 3RD COIL

Pictures of Experimental Setup For Temperature Measurements

The pictures below were taken during an actual temperature experiment. They represent the various components of the setup.

FIGURE A.5 – CONTAINER WITH DRY ICE SURROUND BEAKER OF 100% ETHANOL. THE ETHANOL REACHES TEMPERATURES OF < -50 °C

FIGURE A.6 – GENERAL SETUP OF STEAK AND COOLING PROBE IN THE SCANNER.

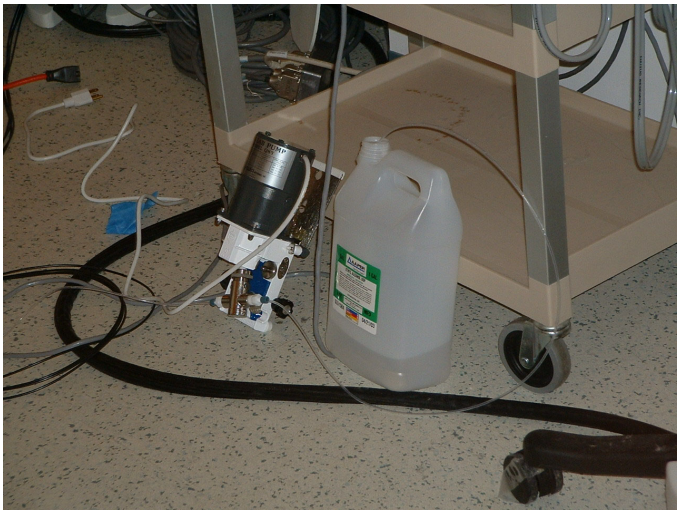

FIGURE A.7 – PUMP AND ETHANOL DUMP (WHERE USED ETHANOL GOES).

FIGURE A.8 – TEMPERATURE MEASUREMENT DEVICE

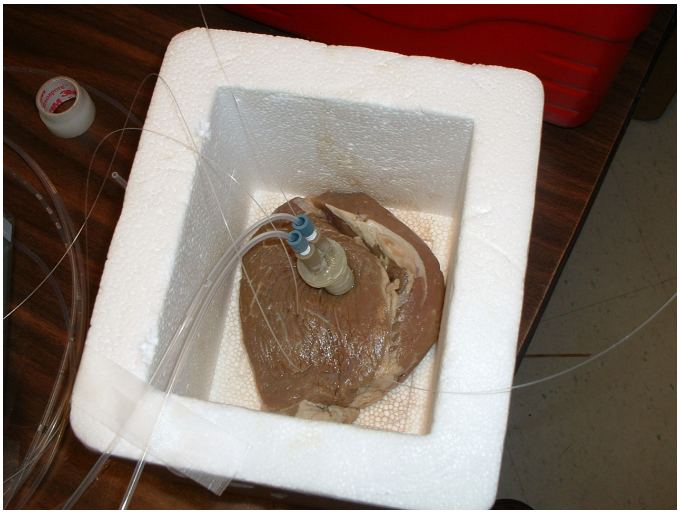

FIGURE A.9 – CLOSE-UP OF ONE TYPE OF THERMOCOUPLE/COOLANT PROBE ARRANGEMENT ON STEAK. THIS SETUP WAS NOT ACTUALLY USED BUT IS SIMILAR IN MOST RESPECTS.

FIGURE A.10 – CLOSE-UP OF FERRULE/NUT COMBINATION USED ON TUBING ENDS TO CONNECT TUBES TO PUMPS AND COOLANT PROBE.

Thermocouple Data For Temperature Experiment

TABLE A.1 – THERMOCOUPLE TEMPERATURE MEASUREMENTS FOR EXPERIMENT SETUP ETHANOL & THREE THERMOCOUPLES.

time (min)	T1	DeltaT1 [deg C]	T2	DeltaT2 [deg C]	T3	DeltaT3 [deg C]
0	17.8	0	14.5	0	13.4	0
0.5	17.8	0	12	-2.5	9.8	-3.6
1	17.6	-0.2	10.1	-4.4	6.7	-6.7
1.5	17.5	-0.3	8.5	-6	4.4	-9

2	17.1	-0.7	6.9	-7.6	2.2	-11.2
2.5	16.9	-0.9	5.5	-9	0.3	-13.1
3	16.6	-1.2	4.4	-10.1	-1.3	-14.7
3.5	16.3	-1.5	3.3	-11.2	-2.7	-16.1
4	16.1	-1.7	2.5	-12	-3.6	-17
4.5	15.7	-2.1	1.5	-13	-4.4	-17.8
5	15.4	-2.4	0.8	-13.7	-5.1	-18.5
5.5	15.2	-2.6	0.2	-14.3	-5.5	-18.9
6	14.8	-3	-0.4	-14.9	-5.7	-19.1
6.5	14.6	-3.2	-1	-15.5	-6	-19.4
7	14.4	-3.4	-1.5	-16	-6.2	-19.6
7.5	14.2	-3.6	-2	-16.5	-6.4	-19.8
8	13.8	-4	-2.4	-16.9	-6.6	-20
8.5	13.5	-4.3	-2.9	-17.4	-7	-20.4
9	13.4	-4.4	-3.1	-17.6	-7	-20.4
9.5	13.1	-4.7	-3.4	-17.9	-7.1	-20.5
10	13	-4.8	-3.6	-18.1	-7.3	-20.7
10.5	12.7	-5.1	-4	-18.5	-7.4	-20.8
11	12.7	-5.1	-4.1	-18.6	-7.4	-20.8
11.5	12.5	-5.3	-4.3	-18.8	-7.5	-20.9
12	12.2	-5.6	-4.5	-19	-7.6	-21
12.5	12.2	-5.6	-4.5	-19	-7.7	-21.1
13	11.9	-5.9	-4.7	-19.2	-7.8	-21.2
13.5	11.7	-6.1	-4.8	-19.3	-7.8	-21.2
14	11.5	-6.3	-5	-19.5	-7.9	-21.3
14.5	11.4	-6.4	-5.1	-19.6	-8	-21.4
15	11.2	-6.6	-5.1	-19.6	-8	-21.4
15.5	11.1	-6.7	-5.1	-19.6	-7.9	-21.3
16	10.9	-6.9	-5.3	-19.8	-8	-21.4
16.5	10.8	-7	-5.4	-19.9	-8	-21.4
17	10.7	-7.1	-5.3	-19.8	-8.1	-21.5
17.5	10.7	-7.1	-5.3	-19.8	-8.1	-21.5
18	10.5	-7.3	-5.5	-20	-8.1	-21.5
18.5	10.5	-7.3	-5.5	-20	-8.1	-21.5
19	10.2	-7.6	-5.5	-20	-8.2	-21.6
19.5	10.2	-7.6	-5.4	-19.9	-8.1	-21.5
20	10.2	-7.6	-5.5	-20	-8.2	-21.6

TABLE A.2 – THERMOCOUPLE TEMPERATURE MEASUREMENTS FOR EXPERIMENT SETUP CHILLED WATER & ONE THERMOCOUPLES.

time (min)	T [deg C]	Delta T [deg C]
0	14.6	0
0.5	14.6	0

1	14.2	-0.4
1.5	13.7	-0.9
2	13.4	-1.2
2.5	13.4	-1.2
3	13.2	-1.4
3.5	12.9	-1.7
4	12.8	-1.8
4.5	12.7	-1.9
5	12.5	-2.1
5.5	12.5	-2.1
6	12.5	-2.1
6.5	12.4	-2.2
7	12.2	-2.4
7.5	12.2	-2.4
8	12.1	-2.5
8.5	12.1	-2.5
9	12	-2.6
9.5	12	-2.6
10	12	-2.6
10.5	11.9	-2.7
11	11.9	-2.7
11.5	11.9	-2.7
12	11.9	-2.7
12.5	11.8	-2.8
13	11.7	-2.9
13.5	11.7	-2.9
14	11.7	-2.9
14.5	11.9	-2.7
15	11.7	-2.9
15.5	11.8	-2.8
16	11.7	-2.9
16.5	11.8	-2.8
17	11.7	-2.9
17.5	11.8	-2.8
18	11.8	-2.8
18.5	11.8	-2.8
19	11.7	-2.9
19.5	11.8	-2.8
20	11.8	-2.8
21	11.8	-2.8
22	11.9	-2.7
23	11.9	-2.7
24	12	-2.6
25	12.1	-2.5
26	12.1	-2.5

27	12.2	-2.4
28	12.2	-2.4
29	12.2	-2.4
30	12.3	-2.3
31	12.4	-2.2
32	12.5	-2.1
33	12.6	-2
34	12.7	-1.9
35	12.8	-1.8
36	12.9	-1.7
37	12.8	-1.8
38	13	-1.6
39	13.1	-1.5
40	13.1	-1.5

Matlab Code For Calculated 2D Temperature Distribution

The Matlab Code below was used to calculated the 2D temperature distributions used in this paper.

```
clear all % Clears all previous variables, etc.

r = 1; % Step Variable For the Rows of the Matrices
c = 1; % Step Variable For the Columns of the Matricies
i = 1;

check = double(dicomread('342')); % check = reference scan for which magnitude is measured.
Use this to filter out bad data points
ref = double(dicomread('352')); % ref = reference scan for which temperature is known
temp1 = double(dicomread('35120')); % temp1 = scan for which temperature is not known
msize = size(ref); % find out the size of the matrix
rows = msize(1,1); % stores the number of rows into the variable rows
columns = msize(1,2); % stores the number of columns into the variable columns
cutoff = 220; % Cutoff for signal intensity
aref = (4096-ref)*pi/2048; % Adjusted Reference Matrice in radians
atemp = (4096-temp1)*pi/2048; % Adjusted Temperature Matrice in radians
lamour = 128; % Lamour frequency in Hz
TE = 0.018; % TE in seconds
reftemp = 0; % reference temperature in Celcius
ambient = 0; % ambient temperature in Celcius
a = 1.221;

while r <= rows

   while c <= columns
```

```
    if check(r,c) <= cutoff
        check(r,c)=-10000;
    end

    c = c + 1;

end


  c = 1;
  r = r + 1;

end

r = 1;
c = 1;

while r <= rows

  while c <= columns

    if check(r,c) ~= -10000

      if abs(atemp(r,c)-aref(r,c)) < a*pi & atemp(r,c) - aref(r,c) < pi/3

        deltatemperature(r,c) = ((-aref(r,c)+atemp(r,c))/(0.01*TE*lamour[2]pi)) + reftemp;

      elseif abs(atemp(r,c)-aref(r,c)) < a*pi & atemp(r,c) - aref(r,c) > pi/3

        deltatemperature(r,c) = ((-aref(r,c)+atemp(r,c)-2*pi)/(0.01*TE*lamour[2]pi)) + reftemp;

      elseif atemp(r,c)-aref(r,c) > a*pi

        deltatemperature(r,c) = ((-aref(r,c)+atemp(r,c)-2*pi)/(0.01*TE*lamour[2]pi)) + reftemp;

      elseif atemp(r,c)-aref(r,c) < -a*pi

        deltatemperature(r,c) = ((-aref(r,c)+atemp(r,c)+2*pi)/(0.01*TE*lamour[2]pi)) + reftemp;

      end

    end

    if check(r,c) == -10000

    deltatemperature(r,c) = ambient;
```

```
      end

       c = c + 1; % Increment the column variable

   end

   c = 1; % Reset the column variable for the next row
   r = r + 1; % Increment the Row Variable.

end

figure
imagesc(deltatemperature)
pixval
colorbar
axis image
```
